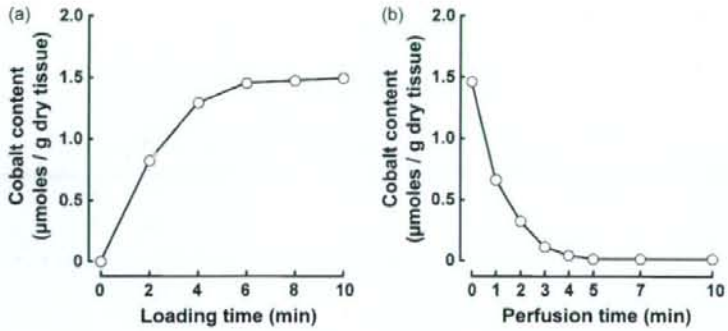

Fig. 1. Time course of changes in tissue cobalt ion content in the cerebral hemisphere of the rat brain perfused for 0 to 10 min with cold Krebs–Henseleit solution containing 1 mM cobalt–EDTA (a) and the time course of changes in tissue cobalt ion distribution of the hemispheres of the rat brain perfused for 8 min with Krebs–Henseleit solution containing 1 mM cobalt–EDTA, followed by further perfusion for 0 to 10 min with a cold washing solution (320 mM mannitol/20 mM Tris/HCl, pH 7.40) (b). The cobalt ion content in the hemisphere was determined by the atomic absorption method.

An animal model with microsphere-induced cerebral embolism was produced by the method described previously [20]. In brief, the blood flow in the right external carotid and the right pterygopalatine arteries were temporarily stopped by ligation. Seven hundred microspheres (diameter of 48 μm, NEN-005, New England Nuclear Inc., Boston, USA) suspended in 20 w/v% dextran solution were injected into the right common carotid artery via a cannula. The rats that underwent a sham operation received the same volume of vehicle without microspheres.

At 15 h after the operation, the neurological deficits of the operated rats were scored based on paucity of movement, truncal curvature, and forced circling during locomotion, which are considered typical symptoms of stroke in rats [20]. Each item was rated from 3 to 0 (3: very severe; 2: severe; 1: moderate; 0: little or none). Rats with a total score of 7–9 points were used in the present study.

Human recombinant HGF was prepared as described earlier [21] and used as a test sample.

The dose of HGF was estimated by the data concerning the dose–response effectiveness of this substance on learning and memory function of the ME animals in previous study [7]. The continuous administration of HGF into the right cerebral ventricle was conducted by injecting a solution of HGF in physiological saline continuously for 3 days into the right cerebral ventricle via an osmotic pressure pump (Alzet model 2001, Alzet, CA, USA) starting from 10 min after injection of the microspheres to the end of treatment, whereby 13 μg of HGF/3 days/animal was administered as described previously [7].

To measure tissue water and cation contents in the intracellular space of the cerebral hemisphere of the rat, we examined a procedure for elimination of extracellular and vascular constituents of non-operated rats (control). We employed a method for perfusion of the brain of the control animal with cobalt–EDTA solution. That is, the rat brain was perfused with a cold Krebs–Henseleit (KH) solution, which additionally contained 1 mM cobalt–EDTA. Perfusion was carried out for different periods of time ranging from 0 to 10 min, and thereafter the tissue water and cation contents were determined according to the dry-weight method and the atomic absorption method, respectively, as described previously [31].

In the next series of experiments, the rat brain was first perfused with the cold KH solution containing 1 mM cobalt–EDTA for 8 min as described above, and then the brain was further perfused with a cold 320 mM mannitol/20 mM Tris/HCl solution, pH 7.4 (washing solution) for 0–10 min at the infusion rate of 9 mL/min. Thereafter, the tissue water and ion contents of the hemispheres were determined according to the atomic absorption method as described previously [31].

The time period for measurement of tissue water and ion contents (day 3 after ME) was decided on the basis of the following data reported previously; (1) the FITC-albumin leakage, an indicator of disruption of the BBB [6], of the ME animals was detectable from day 1 to day 7 with the maximal leakage being on day 3 [7]; (2) the content of occludin and ZO-1, both tight junctional proteins of the BBB, was decreased on days 1–3 after ME [14]; and (3) the infarct area detected by hematoxylin–eosin staining was almost completely developed by 3–7 days after ME [20]. These results suggest the possibility that disruption of the BBB and formation of ischemic cerebral edema in rats with ME occur, at the latest, at 3 days after ME.

Statistical significance was evaluated by a Student's *t*-test when two groups were compared, and by analysis of variance (ANOVA) followed by post hoc Fisher's protected least significant difference test when multiple groups were compared. Differences with a probability of 5% or less were considered significant ($P < 0.05$).

In the case of the HGF treatment study, 80% (8/10) of the microsphere-administered animals had neurological deficits with a total score of 7–9 points and the remaining 20% (2/10) of them, a total score of 4–6 points at 15 h after ME. The Sham animal did not reveal any stroke-like symptoms throughout the experiment.

At first, we determined how fast the cobalt–EDTA was distributed to the cerebral hemisphere. Fig. 1a shows the time course of changes in the cobalt ion content of the right hemisphere of control (naïve) rats that had been perfused with KH solution containing 1 mM cobalt–EDTA pre-equilibrated with a gas mixture of 95% O_2 and 5% CO_2, pH 7.4. A rapid increase in the cobalt–EDTA content during 0–4 min of perfusion and a gradual increase in the cobalt ion content during 4–8 min of perfusion were seen. Almost the maximal value was achieved by 8 min of the perfusion. Next, we determined how the cobalt–EDTA disappeared from the brain. Fig. 1b shows the time course of disappearance of tissue cobalt ions from the brain hemisphere that had been perfused for 8 min with the cold KH solution containing 1 mM cobalt–EDTA, as shown above. A rapid decrease and, thereafter, a gradual decrease in cobalt–EDTA from the brain, were seen. Almost complete disappearance of the cobalt–EDTA was detected after 5 min of perfusion. These results indicate that 5 min perfusion with the cold, isotonic, washing solution is suitable for assessing the tissue ion content excluding those present in the extracellular and vascular spaces.

According to the results on perfusion study just described, we employed a procedure for determination of tissue water and ion contents of the brain after perfusion with the cold washing solution for 5 min at an infusion rate of 9.0 mL/min.

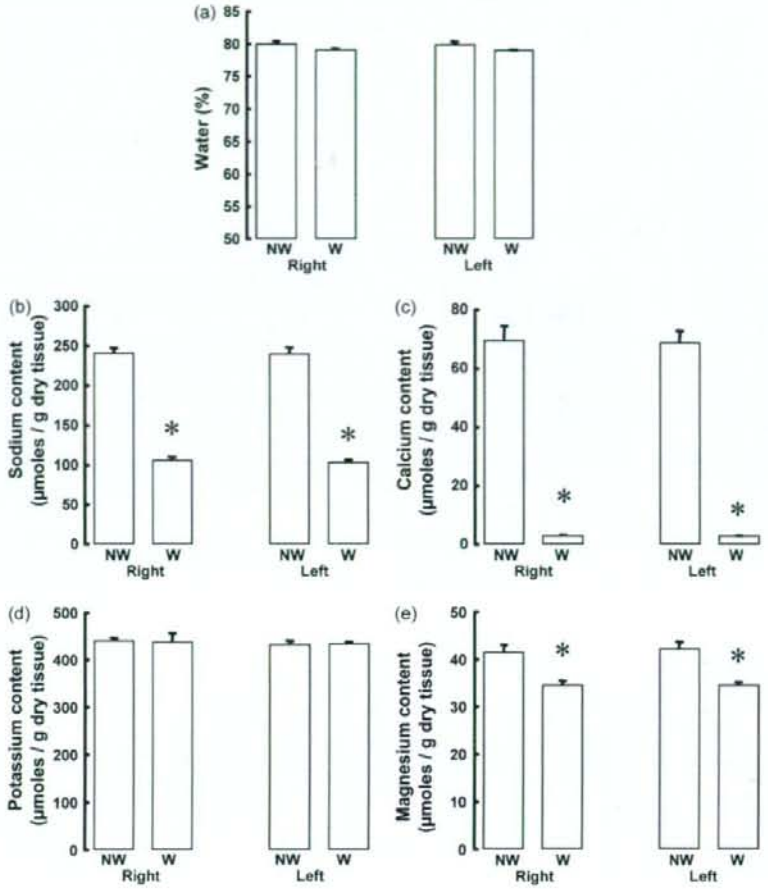

Fig. 2. Comparison of tissue water and ion contents of the right and left hemispheres of the control rat perfused via the heart for 5 min (W) or non-perfused (NW) with the washing solution (320 mM mannitol/20 mM Tris/HCl, pH 7.4). Each value represents the mean ± S.E.M. of three experiments. *Significantly different from non-washing group ($p < 0.05$).

Fig. 2 shows a comparison of tissue water and ion contents of control rat brains determined by the current method with washing and non-washing procedures. Significant differences in tissue sodium, calcium, and magnesium ion contents between them were seen, whereas tissue water and potassium ion contents did not differ between the two groups.

Fig. 3 shows tissue water contents of the brain of control, sham-operated, HGF-untreated ME, and HGF-treated ME rats on day 3 after ME. There was a substantial increase in the tissue water content of the right hemisphere of the ME animal. This increase was significantly attenuated by treatment with HGF [ANOVA: $F(3,11) = 65.386$, $P < 0.0001$]; Fisher's PLSD: Sham vs. ME: $P < 0.0001$; ME vs. HGF, $P < 0.01$]. A significant, but slight, increase in the water content in the left hemisphere of the ME rat was detected. This increase was almost completely suppressed by the treatment with HGF [ANOVA: $F(3,11) = 4.402$, $P < 0.05$; Fisher's PLSD: Sham vs. ME, $P < 0.01$; ME vs. HGF, $P < 0.05$].

Fig. 4a–d shows changes in tissue sodium, calcium, potassium, and magnesium ion contents, respectively, of the right and left hemispheres of the control, sham-operated, HGF-untreated ME, and HGF-treated ME animals on day 3. A marked increase in sodium ion content of the right hemisphere of the ME rat was observed. This increase was partially attenuated by treatment with HGF [ANOVA: $F(3,11) = 187.550$, $P < 0.0001$; Fisher's PLSD: Sham vs. ME, $P < 0.0001$; ME vs. HGF, $P < 0.05$]. There was a slight, but significant, increase in the sodium ion content of the left hemisphere of the ME rat and this increase was completely attenuated by the treatment with HGF [ANOVA: $F(3,11) = 5.794$, $P < 0.05$; Fisher's PLSD: Sham vs. ME, $P < 0.01$; ME vs. HGF, $P < 0.05$].

The tissue calcium ion content in the right hemisphere was increased in response to ME, and this increase was partially attenuated by treatment with HGF [ANOVA: $F(3,11) = 204.087$, $P < 0.0001$; Fisher's PLSD: Sham vs. ME, $P < 0.0001$; ME vs. HGF, $P < 0.001$].

There were significant decreases in potassium and magnesium ion contents of the right hemisphere of the ME rat, and these decreases were not attenuated by treatment with HGF. Two-way ANOVA followed by Fisher's PLSD test showed no significant difference in the sodium, calcium, potassium, and magnesium ion contents of the right and left hemispheres between control and sham-operated rats.

In the present study, the rat brains were subjected to the washing procedure using an isotonic mannitol solution to avoid the influence of the extracellular and vascular constituents on the total tissue ion content determined. A preferable movement of cobalt

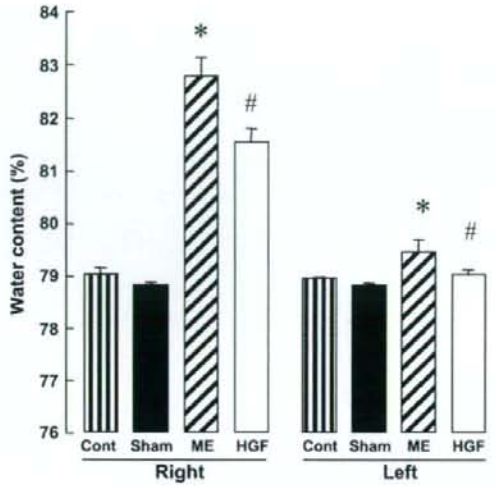

Fig. 3. Effects of HGF treatment on the brain water content of HGF-untreated (ME) and HGF-treated (HGF) rats with microsphere embolism. 'Cont' indicates non-operated animal and 'Sham', sham-operated animal. Each value represents the mean ± S.E.M. of three (Cont) or four (Sham, ME, and HGF) experiments. #Significantly different from Sham group; *significantly different from ME group ($p < 0.05$).

ion between intra- and extra-cellular spaces, that is, saturation of cobalt ion in the brain tissue during perfusion with KH solution for 8 min and the following gradual washout of this ion for 5 min by the isotonic mannitol solution were detected. There were significant differences in tissue sodium, calcium, and magnesium ion contents between washed and non-washed brains, suggesting a significant contribution of the extracellular and vascular constituents to the total tissue ion contents determined. Particularly, the tissue calcium ion content of the washed hemisphere was 1/20th of the total tissue calcium ion content of the non-washed hemisphere; and the total tissue sodium ion, 2/5th of the total tissue sodium ion content of the non-washed hemisphere. These results suggest a large contribution of the extracellular and vascular constituents to these ion contents if determined without the washing procedure. Since we observed no significant differences in the tissue water or potassium ion contents between the washed and non-washed brains of control rats, the washing procedure is unlikely to non-specifically alter the permeability of tissue constituents through the BBB. Thus, this procedure could be utilizable for the assessment of pathophysiological alterations in the intracellular water and ions.

It is generally believed that loss of ion homeostasis plays a central role in the pathogenesis of ischemic cell damage in the brain. Ischemia-induced perturbation of ion homeostasis leads to the intracellular accumulation of sodium and calcium ions, followed by subsequent activation of proteases and phospholipases and the formation oxygen and nitrogen free radicals [16]. Consequently, these events cause functional and structural changes including cerebral

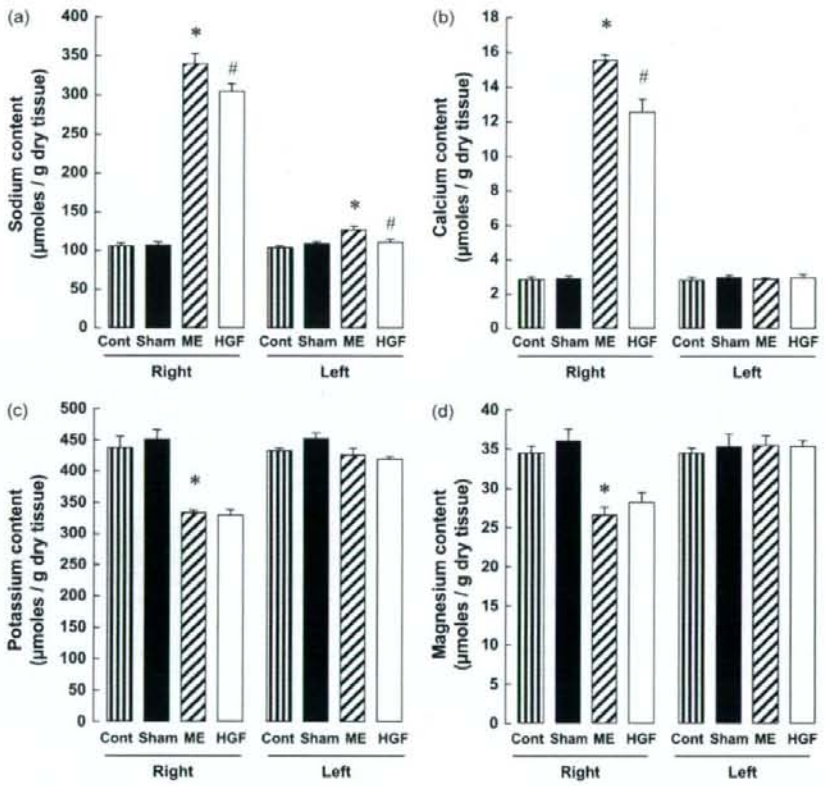

Fig. 4. Effects of HGF treatment on the brain sodium, calcium, potassium, and magnesium ion contents in both hemispheres of HGF-untreated (ME) and HGF-treated (HGF) rats with microsphere embolism. 'Cont' indicates non-operated animals; and 'Sham', sham-operated animals. Each value represents the mean ± S.E.M. of three (Cont) or four (Sham, ME, and HGF) experiments. #Significantly different from the Sham group and *significantly different from ME group ($p < 0.05$).

edema and eventually lead to cell death. Consistent with the above ischemic cell death, ME in the current study induced an increase in the water content, a sign of cerebral edema [15], of the ipsilateral hemisphere of the animal, which elevation was associated with increases in the tissue sodium and calcium ion contents and decreases in the tissue potassium and magnesium ion contents. Since the total tissue ion contents determined in the present experiment excluded constituents present in vascular and extracellular spaces, the results may represent substantial alteration of ions in the intracellular space of the hemisphere of the ME rat, which may be involved in the genesis of ischemic cerebral edema. Interestingly, we observed that the ME-induced ionic disturbances were almost the same as those in the intracellular sodium, calcium, and potassium ion contents in the ischemic/reperfused heart [30]. It is generally believed as a mechanism responsible for ionic disturbances in the ischemic/reperfused heart that sodium ion overload during ischemia is increased due to an ATP breakdown-stimulated increase in H^+ formation and energy production failure-induced inhibition of Na^+, K^+-ATPase activity, followed by augmentation of Na^+/H^+ exchanger activity during ischemia and that calcium ion overload during postischemic reperfusion is enhanced due to an increase in the calcium entry-mode Na^+/Ca^{2+} exchanger activity. This notion is consistent with the reports of several investigators on the ionic perturbation in neuronal and glial cells that occurred due to alterations in Na^+, K^+-ATPase [9], Na^+/H^+ exchanger [3,4], Na^+/Ca^{2+} exchanger [4,18,33] and Na^+–K^+–Cl^--cotransporter [5] in the brain.

Continuous treatment for 3 days with human recombinant HGF resulted in a partial attenuation of the alterations in water, sodium, calcium, and potassium ion contents. The results in the current experiments suggest that HGF-treatment was capable of attenuating the brain edema that occurred within 3 days after the cerebral embolism. As described earlier, we observed that HGF attenuated FITC-albumin leakage [7] and decreases in the expression of tight junctional proteins, occludin and ZO-1, in the endothelial cells after ME [8]. Although further studies on the mechanisms responsible for the effects of HGF on the ischemic cerebral edema are required, the present results demonstrated inhibition of the increases in sodium and calcium and water contents as a possible mechanism for the protective effect of HGF against ME-induced brain injury.

Acknowledgment

This work was supported in part by the Promotion and Mutual Aid Corporation for Private Schools of Japan.

References

[1] C.L. Achim, S. Katyal, C.A. Wiley, M. Shiratori, G. Wang, E. Oshika, B.E. Petersen, J.M. Li, G.K. Michalopoulos, Expression of HGF and cMet in the developing and adult brain, Brain Res. Dev. Brain Res. 102 (1997) 299–303.
[2] S. Avery, H.A. Crockard, R.R. Russell, Evolution and resolution of oedema following severe temporary cerebral ischaemia in the gerbil, J. Neurol. Neurosurg. Psychiatry 47 (1984) 604–610.
[3] I.A. Bobulescu, F. Di Sole, O.W. Moe, Na^+/H^+ exchangers: physiology and link to hypertension and organ ischemia, Curr. Opin. Nephrol. Hypertens. 14 (2005) 485–494.
[4] A. Bondarenko, N. Svichar, M. Chesler, Role of Na^+–H^+ and Na^+–Ca^{2+} exchange in hypoxia-related acute astrocyte death, Glia 49 (2005) 143–152.
[5] J. Brillault, T.I. Lam, J.M. Rutkowsky, S. Foroutan, M.E. O'Donnell, Hypoxia effects on cell volume and ion uptake of cerebral microvascular endothelial cells, Am. J. Physiol. Cell Physiol. 294 (2008) C88–96.
[6] M. Cavaglia, S.M. Dombrowski, J. Drazba, A. Vasanji, P.M. Bokesch, D. Janigro, Regional variation in brain capillary density and vascular response to ischemia, Brain Res. 910 (2001) 81–93.
[7] I. Date, N. Takagi, K. Takagi, T. Kago, K. Matsumoto, T. Nakamura, S. Takeo, Hepatocyte growth factor attenuates cerebral ischemia-induced learning dysfunction, Biochem. Biophys. Res. Commun. 319 (2004) 1152–1158.
[8] I. Date, N. Takagi, K. Takagi, K. Tanonaka, H. Funakoshi, K. Matsumoto, T. Nakamura, S. Takeo, Hepatocyte growth factor attenuates cerebral ischemia-induced increase in permeability of the blood–brain barrier and decreases in expression of tight junctional proteins in cerebral vessels, Neurosci. Lett. 407 (2006) 141–145.
[9] S. Decollogne, I.B. Bertrand, M. Ascensio, I. Drubaix, L.G. Lelievre, Na^+, K^+-ATPase and Na^+/Ca^{2+} exchange isoforms: physiological and physiopathological relevance, J. Cardiovasc. Pharmacol. 22 (Suppl. 2) (1993) S96–98.
[10] O. Gotoh, T. Asano, T. Koide, K. Takakura, Ischemic brain edema following occlusion of the middle cerebral artery in the rat. I. The time courses of the brain water, sodium and potassium contents and blood–brain barrier permeability to 125I-albumin, Stroke 16 (1985) 101–109.
[11] S. Honda, M. Kagoshima, A. Wanaka, M. Tohyama, K. Matsumoto, T. Nakamura, Localization and functional coupling of HGF and c-Met/HGF receptor in rat brain: implication as neurotrophic factor, Mol. Brain Res. 32 (1995) 197–210.
[12] K.A. Hossmann, F.J. Schuier, Experimental brain infarcts in cats. I. Pathophysiological observations, Stroke 11 (1980) 583–592.
[13] R.C. Janzer, M.C. Raff, Astrocytes induce blood–brain barrier properties in endothelial cells, Nature 325 (1987) 253–257.
[14] T. Kago, N. Takagi, I. Date, Y. Takenaga, K. Takagi, S. Takeo, Cerebral ischemia enhances tyrosine phosphorylation of occludin in brain capillaries, Biochem. Biophys. Res. Commun. 339 (2006) 1197–1203.
[15] R. Katzman, R. Clasen, I. Klatzo, J.S. Meyer, H.M. Pappius, A.G. Waltz, Report of Joint Committee for Stroke Resources. IV. Brain edema in stroke, Stroke 8 (1977) 512–540.
[16] D.B. Kintner, Y. Wang, D. Sun, Role of membrane ion transport proteins in cerebral ischemic damage, Front. Biosci. 12 (2007) 762–770.
[17] K. Kogure, R. Busto, P. Scheinberg, The role of hydrostatic pressure in ischemic brain edema, Ann. Neurol. 9 (1981) 273–282.
[18] D.G. MacGregor, M.V. Avshalumov, M.E. Rice, Brain edema induced by in vitro ischemia: causal factors and neuroprotection, J. Neurochem. 85 (2003) 1402–1411.
[19] K. Matsumoto, T. Nakamura, Hepatocyte growth factor (HGF) as a tissue organizer for organogenesis and regeneration, Biochem. Biophys. Res. Commun. 239 (1997) 639–644.
[20] K. Miyake, S. Takeo, H. Kajihara, Sustained decrease in brain regional blood flow after microsphere embolism in rats, Stroke 24 (1993) 415–420.
[21] T. Nakamura, T. Nishizawa, M. Hagiya, T. Seki, M. Shimonishi, A. Sugimura, K. Tashiro, S. Shimizu, Molecular cloning and expression of human hepatocyte growth factor, Nature 342 (1989) 440–443.
[22] M. Niimura, N. Takagi, K. Takagi, R. Mizutani, N. Ishihara, K. Matsumoto, H. Funakoshi, T. Nakamura, S. Takeo, Prevention of apoptosis-inducing factor translocation is a possible mechanism for protective effects of hepatocyte growth factor against neuronal cell death in the hippocampus after transient forebrain ischemia, J. Cereb. Blood Flow Metab. 26 (2006) 1354–1365.
[23] M.A. Petty, E.H. Lo, Junctional complexes of the blood–brain barrier: permeability changes in neuroinflammation, Prog. Neurobiol. 68 (2002) 311–323.
[24] S. Rush, G. Khan, A. Bamisaiye, P. Bidwell, H.A. Leaver, M.T. Rizzo, c-Jun amino-terminal kinase and mitogen activated protein kinase 1/2 mediate hepatocyte growth factor-induced migration of brain endothelial cells, Exp. Cell Res. 313 (2007) 121–132.
[25] W. Sun, H. Funakoshi, T. Nakamura, Localization and functional role of hepatocyte growth factor (HGF) and its receptor c-met in the rat developing cerebral cortex, Mol. Brain Res. 103 (2002) 36–48.
[26] N. Takagi, K. Miyake, T. Taguchi, H. Tamada, K. Takagi, N. Sugita, S. Takeo, Failure in learning task and loss of cortical cholingergic fibers in microsphere-embolized rats, Exp. Brain Res. 114 (1997) 279–287.
[27] N. Takagi, H. Tsuru, M. Yamamura, S. Takeo, Changes in striatal dopamine metabolism after microsphere embolism in rats, Stroke 26 (1995) 1101–1106.
[28] S. Takeo, K. Miyake, R. Minematsu, K. Tanonaka, M. Konishi, In vitro effect of naftidrofuryl oxalate on cerebral mitochondria impaired by microsphere-induced embolism in rats, J. Pharmacol. Exp. Ther. 248 (1989) 1207–1214.
[29] S. Takeo, K. Miyake, K. Tanonaka, R. Tanonaka, T. Taguchi, K. Okano, K. Inoue, Y. Ohga, Y. Kishimoto, Time course of changes in brain energy metabolism of the rat after microsphere-induced cerebral embolism, Jpn. J. Pharmacol. 55 (1991) 197–209.
[30] S. Takeo, K. Tanonaka, Na^+ overload-induced mitochondrial damage in the ischemic heart, Can. J. Physiol. Pharmacol. 82 (2004) 1033–1043.
[31] K. Tanonaka, A. Takasaki, H. Kajiwara, S. Takeo, Contribution of sodium channel and sodium/hydrogen exchanger to sodium accumulation in the ischemic myocardium, Gen. Pharmacol. 34 (2000) 167–174.
[32] N.V. Todd, P. Picozzi, A. Crockard, R.W. Russell, Duration of ischemia influences the development and resolution of ischemic brain edema, Stroke 17 (1986) 466–471.
[33] A. Tortiglione, B. Picconi, I. Barone, D. Centonze, S. Rossi, C. Costa, M. Di Filippo, A. Tozzi, M. Tantucci, G. Bernardi, L. Annunziato, P. Calabresi, Na^+/Ca^{2+} exchanger maintains ionic homeostasis in the peri-infarct area, Stroke 38 (2007) 1614–1620.

Available online at www.sciencedirect.com
ScienceDirect
Experimental Neurology 210 (2008) 83 – 94
Experimental Neurology
www.elsevier.com/locate/yexnr

Hepatocyte growth factor improves synaptic localization of the NMDA receptor and intracellular signaling after excitotoxic injury in cultured hippocampal neurons

Hiromi Akita [a], Norio Takagi [a,*], Naoko Ishihara [a], Keiko Takagi [a], Kazutoshi Murotomi [a], Hiroshi Funakoshi [b], Kunio Matsumoto [b,1], Toshikazu Nakamura [b], Satoshi Takeo [a]

[a] *Department of Molecular and Cellular Pharmacology, Tokyo University of Pharmacy and Life Sciences, 1432-1 Horinouchi, Hachioji, Tokyo 192-0392, Japan*
[b] *Division of Molecular Regenerative Medicine, Department of Biochemistry and Molecular Biology, Osaka University Graduate School of Medicine, 2-2-B7 Yamadaoka, Suita, Osaka 565-0871, Japan*

Received 23 May 2007; revised 6 September 2007; accepted 4 October 2007
Available online 13 October 2007

Abstract

To examine the effects of HGF on synaptic densities under excitotoxic conditions, we investigated changes in the number of puncta detected by double immunostaining with NMDA receptor subunits and presynaptic markers in cultured hippocampal neurons. Exposure of hippocampal neurons to excitotoxic NMDA (100 μM) decreased the synaptic localization of NMDA receptor subunit NR2B, whereas synaptic NR1 and NR2A clusters were not altered. Colocalization of PSD-95, a scaffolding protein of the receptor, with the presynaptic protein synapsin I was also decreased after excitotoxicity. Treatment with HGF attenuated these decreases in number. The decrease in the levels of surface NR2B subunits following the addition of the excitotoxic NMDA was also attenuated by the HGF treatment. The decrease in CREB phosphorylation in response to depolarization-evoked NMDA receptor activation was prevented by the HGF treatment. These results suggest that HGF not only prevented neuronal cell death but also attenuated the decrease in synaptic localization of NMDA receptor subunits and prevented intracellular signaling through the NMDA receptor.

Keywords: Hepatocyte growth factor; Neuronal injury; *N*-methyl-D-aspartate receptor; PSD-95

Introduction

The *N*-methyl-D-aspartate (NMDA) receptor, a subtype of ionotropic glutamate receptors, is highly permeable to Ca^{2+} and Na^{+} (Dale and Roberts, 1985) and plays a pivotal role in the regulation of neuronal development, learning and memory, and neurodegenerative diseases (Dingledine et al., 1999). NMDA receptors are heteromeric complexes of NR1 and 4 types of NR2 (NR2A-2D), or NR3 subunits (Das et al., 1998; Ishii et al., 1993; Monyer et al., 1992; Moriyoshi et al., 1991; Nakanishi, 1992; Nishi et al., 2001). Whereas NR1 is the principal subunit for the channel activity of the NMDA receptor, the NR2 subunits serve to modulate the properties of these heteromeric receptors (Hollmann and Heinemann, 1994).

The postsynaptic density (PSD), which underlies the postsynaptic membrane at excitatory synapses, has been implicated in the linkage of receptors to signaling proteins and to the cytoskeleton (Kennedy, 1997; Kim and Sheng, 2004; Klauck and Scott, 1995; Ziff, 1997). PSD-95, a major protein component of the PSD, interacts with NMDA receptor subunits NR2A and NR2B by binding between PDZ (postsynaptic density-95, PSD-95/Discs large, Dlg/zona occludens-1, ZO-1) domains of PSD-95 and the C-terminal PDZ-binding motif of the receptor proteins (Cho et al., 1992; Kim and Sheng, 2004). PSD-95 also binds to signaling proteins such as neuronal nitric oxide synthase (Brenman et al., 1996) and synaptic Ras-GTPase activating protein p135synGAP (Chen et al., 1998; Kim et al., 1998) and organizes these intracellular signaling complexes. Therefore, it has been implied that PSD-95 links the NMDA receptor to intracellular

Abbreviations: CNQX, 6-cyano-7-nitro-quinoxaline-2,3-dione; CREB, cAMP-response-element-binding protein; HGF, hepatocyte growth factor; NMDA, *N*-methyl-D-aspartate; PI, propidium iodide; PSD, postsynaptic density.

* Corresponding author.
E-mail address: takagino@ps.toyaku.ac.jp (N. Takagi).
[1] Present address: Division of Tumor Dynamics and Regulation, Cancer Research Institute, Kanazawa University, Kanazawa, Japan.

0014-4886/$ - see front matter © 2007 Elsevier Inc. All rights reserved.
doi:10.1016/j.expneurol.2007.10.001

signaling pathways at the synapse and plays an important role in synaptic plasticity and learning. With regard to this, in mice carrying a targeted mutation in their PSD-95 gene, NMDA receptor-mediated synaptic plasticity was altered and spatial learning in a water maze was impaired (Migaud et al., 1998).

In contrast to the crucial roles of the NMDA receptor in physiological activities such as learning and memory, an excessive activation of the receptor has been associated with diverse neurological and neurodegenerative disorders, including cerebral ischemia, epilepsy, Parkinson's disease, Alzheimer's disease, Huntington's chorea, and amyotrophic lateral sclerosis (Dingledine et al., 1999). Therefore, it has become an important objective to investigate strategies to protect cells from NMDA receptor-mediated excitotoxicity. The hepatocyte growth factor (HGF), which was found to be a potent mitogen for hepatocytes (Nakamura et al., 1984, 1989), acts as an organotrophic factor for regeneration and has a protective effect in various organs (Balkovetz and Lipschutz, 1999; Matsumoto and Nakamura, 1996; Matsumoto and Nakamura, 2001; Zarnegar and Michalopoulos, 1995). In addition, HGF is known to evoke diverse cellular responses, including motogenic, morphogenic, angiogenic, and anti-apoptotic activities in various types of cells (Matsumoto and Nakamura, 1996; Nakamura et al., 1989; Thompson et al., 2004; Zarnegar and Michalopoulos, 1995). In the central nervous system, HGF and its c-Met receptor were found to function in a variety of ways (Achim et al., 1997; Honda et al., 1995; Sun et al., 2002a,b), including protection of tyrosine hydroxylase-positive midbrain neurons, as well as hippocampal and cortical neurons, against aging-related cell death in culture (Hamanoue et al., 1996; Honda et al., 1995; Machide et al., 1998). We recently demonstrated that HGF prevented *in vivo* ischemic brain injuries (Date et al., 2004; Niimura et al., 2006). Furthermore, HGF improved learning and memory dysfunction of ischemic rats in our previous study (Date et al., 2004). Although HGF exerts protective effects on cultured hippocampal neurons under pathophysiological conditions (Ishihara et al., 2005), it is still not clear whether HGF affects synaptic function of neurons under such conditions. In the present study, to achieve further insight into the reason for the potency of HGF treatment, we examined the effect of HGF on synaptic clustering of NMDA receptor subunits and PSD-95 in hippocampal neurons after excitotoxic injury. To assess the biochemical response to excitatory input, we furthermore evaluated the phosphorylation of cAMP-response-element-binding protein (CREB) mediated by the NMDA receptor. The results obtained show that HGF not only prevented the decrease in the number of synaptic NMDA receptor subunits and PSD-95 but also attenuated the decrease in the surface expression of NDMA receptor subunits. Furthermore, HGF improved phosphorylation of CREB in response to depolarization-evoked activation of the NMDA receptor.

Experimental procedures

Primary hippocampal cell cultures

Primary hippocampal cell cultures were prepared from fetal rats at gestational day 18 as described previously (Huettner and Baughman, 1986), with slight modifications (Ishihara et al., 2005). Brains were dissected out and the pooled hippocampi were dissociated by incubation at 37 °C for 30 min in Hank's balanced salt solution containing 15 U/ml papain, 210 U/ml deoxyribonuclease I, 1 mM L-cysteine, and 0.5 mM EDTA. The dispersed cells were resuspended in Dulbecco's Modified Eagle's Medium containing 10% horse serum, and plated at a density of 40,000 cells/cm^2 on 12-well plates or in 35-mm dishes coated with poly-L-lysine. At 24 h after plating, the medium was replaced with serum-free Neurobasal medium containing 2% B27 supplement (Gibco-BRL, Rockville, MD, USA) and 0.5 mM glutamine. To inhibit proliferation of non-neuronal cells, we added cytosine arabinoside (1 μM) to each plate or dish. At 3 and 10 days *in vitro* (DIV), one-half of the medium was replaced with fresh Neurobasal medium having the 2% B27 supplement and 0.5 mM glutamine. Cultures were maintained at 37 °C in a 5% CO_2 incubator and used for experiments at 15–18 DIV.

For the experiment of high K^+-induced CREB phosphorylation, 10 μM 6-cyano-7-nitro-quinoxaline-2,3-dione (CNQX), 10 μM nifedipine, and 0.3 μM TTX were added 30 min before treatment with 57 mM KCl to inhibit AMPA receptors, L-type calcium channels, and spontaneous synaptic activity, respectively. Hippocampal cells were depolarized for 3 min with 10 mM HEPES buffer, pH 7.4, containing 60 mM KCl, 67 mM NaCl, 2 mM $CaCl_2$–$2H_2O$, 10 mM D-glucose, 10 μM glycine, 10 μM CNQX, 10 μM nifedipine, and 0.3 μM TTX. To inhibit the NMDA receptor, we added 10 μM MK-801 to cultures in some experiments.

Recombinant HGF

Human recombinant HGF was purified from conditioned medium of Chinese hamster ovary cells transfected with an expression vector containing human HGF cDNA as described earlier (Nakamura et al., 1989). The purity of hrHGF was >98%, as determined by SDS-PAGE.

Cell viability assay

Hippocampal cells were washed twice with 10 mM HEPES buffer, pH 7.4, containing 144 mM NaCl, 2 mM $CaCl_2$, 1 mM $MgCl_2$, 5 mM KCl, and 10 mM D-glucose and were then incubated for 15 min at 37 °C in a 5% CO_2 incubator with 100 μM NMDA in 10 mM HEPES buffer, pH 7.4, containing 144 mM NaCl, 2 mM $CaCl_2$, 5 mM KCl, 10 mM D-glucose, and 10 μM glycine. The hippocampal cells were then washed and maintained in Neurobasal medium containing 2% B27 supplement and 0.5 mM glutamine. After 1, 6 or 24 h of incubation, the cells were incubated with 2 μg/ml propidium iodide (PI) for 20 min. After having been washed with phosphate-buffered saline, cells were fixed in 4% paraformaldehyde to determine the total number of neurons by immunostaining with anti-microtubule-associated protein 2 (MAP-2) antibody. Fluorescent images of cells were captured by a CCD camera (DP50, Olympus, Tokyo, Japan) mounted on an Olympus BX52 microscope equipped with a mercury arc lamp. The number of PI- or MAP-2-positive cells was counted in 10 randomly

chosen areas (245×320 μm) of each well. Results were obtained from 10 frames in 4 wells in 4 independent experiments. HGF was added at the concentration of 30 ng/ml 1 h before the addition of NMDA. The microscopic observations were performed by a person unaware of the study group.

Immunohistochemistry

After having been fixed with ice-cold methanol and blocked, the cells were incubated with the primary antibody, and then with the secondary antibody in blocking solution. They were then incubated with another primary antibody and subsequently with the corresponding secondary antibody. For double immunostaining of mouse anti-NR1 or mouse anti-NR2B antibody with rabbit anti-synapsin antibody, the cells were incubated overnight at 4 °C with mouse anti-NR1 or anti-NR2B antibody (BD Biosciences) and then with biotinylated anti-mouse IgG (Vector Laboratories) for 2 h and streptavidin FITC for 1 h. The cells were incubated with rabbit anti-synapsin I antibody, another primary antibody, for 1 h at 37 °C and subsequently with Cy3-conjugated donkey anti-rabbit IgG (Jackson Immunoresearch) for 1 h at 37 °C. For double immunostaining of mouse anti-PSD-95 antibody with anti-synapsin antibody, the cells were incubated with mouse anti-PSD-95 antibody for 1 h at 37 °C and then with FITC-conjugated goat anti-mouse IgG (ICN Pharmaceutical, Inc.). The cells were incubated with rabbit anti-synapsin I antibody, another primary antibody, for 1 h at 37 °C and subsequently with Cy3-conjugated donkey anti-rabbit IgG (Jackson Immunoresearch) for 1 h at 37 °C. Since we could not obtain commercially available mouse anti-NR2A antibody for double immunostaining with rabbit anti-synapsin I antibody, we decided to use rabbit anti-NR2A antibody. In this regard, we used mouse anti-synaptotagmin antibody as a presynaptic marker, since attempts to examine immunostaining of synapsin I using commercially available mouse anti-synapsin I antibody were not successful under conditions in the present study. To provide evidence about the similarity of the two presynaptic markers synapsin and synaptotagmin, we examined double immunostaining of synapsin with synaptotagmin. The cells were incubated with rabbit anti-synapsin I antibody and subsequently with Cy3-conjugated donkey anti-rabbit IgG (Jackson Immunoresearch). The cells were incubated with mouse anti-synaptotagmin antibody, another antibody, for 1 h at 37 °C and subsequently with FITC-conjugated goat anti-mouse IgG (Jackson Immunoresearch). For double immunostaining of NR2A with synaptotagmin, the cells were incubated overnight at 25 °C with rabbit anti-NR2A antibody and then with biotinylated anti-rabbit IgG (Vector Laboratories) for 2 h and streptavidin FITC for 1 h at 37 °C. The cells were incubated with mouse anti-synaptotagmin antibody, another antibody, for 1 h at 37 °C and subsequently with Cy3-conjugated goat anti-mouse IgG (Jackson Immunoresearch) for 1 h at 37 °C. Fluorescent images of cells were captured by a CCD camera (DP50) mounted on an Olympus BX52 microscope equipped with a mercury arc lamp. Images were processed by using Adobe Photoshop (Adobe Systems, Mountain View, CA). To count the number of clusters, we evaluated at least 1 dendrite (50 μm length) in each of 5 randomly selected cells in each of 5 separate cultures. The number of immunolabeled puncta with each antibody and double-immunolabeled puncta on basal dendritic segments were manually counted. The microscopic observations were performed by a person unaware of the study group.

Cell-surface biotinylation assay

Surface biotinylation of hippocampal neurons was performed as described previously (Shen et al., 2000) with minor modifications. Hippocampal neurons in culture were washed 3 times with ice-cold PBS, pH 7.4, containing 10 mM Na_2HPO_4, 2.7 mM KCl, 137 mM NaCl, 1.0 mM $CaCl_2$, and 0.5 mM $MgCl_2$. Surface proteins were then biotinylated with 1.0 mg/ml sulfo-NHS-SS-biotin (Pierce, Rockford, IL) for 20 min in PBS at 4 °C. For removal of unreacted sulfo-NHS-SS-biotin, cells were washed 3 times with ice-cold 50 mM Tris/PBS, pH 7.4, containing 10 mM Na_2HPO_4, 2.7 mM KCl, 137 mM NaCl, 1.0 mM $CaCl_2$, and 0.5 mM $MgCl_2$. The cells were then lysed

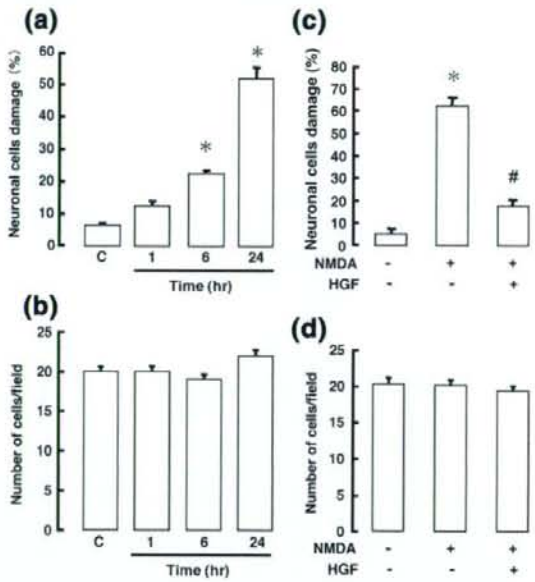

Fig. 1. Time course of changes in NMDA-induced excitotoxic damage to cultured hippocampal cells and the effects of HGF on the damage. (a and b) Hippocampal cells were treated with 100 μM NMDA for 15 min and then incubated in normal conditioned medium without NMDA for 1, 6 or 24 h and thereafter stained with propidium iodide (PI) to detect injured cells and anti-MAP-2 antibody to identify neurons. The number of PI-labeled cells (a) was normalized by total number of MAP-2-positive neurons (b) within the same field (245×320 μm). "C" indicates incubation under normal culture conditions for 24 h without NMDA treatment. (c and d) Cultured hippocampal cells were pretreated or not with 30 ng/ml HGF for 1 h before the addition of 100 μM NMDA. Then, the cells were incubated in normal conditioned medium without NMDA for 24 h. The number of PI-labeled cells (c) was normalized by the total number of MAP-2-positive neurons (d) within the same field (245×320 μm). Results are the means±SEM from 10 fields in 4 wells in 4 independent experiments. *Significant difference from the control group (post hoc Dunnet's *t*-test in a; post hoc Fisher's PLSD in c; $p<0.05$). #Significant difference from the NMDA-treated group (post hoc Fisher's PLSD, $p<0.05$).

with ice-cold lysis buffer (10 mM sodium phosphate, pH 7.4, containing 100 mM NaCl, 0.2% SDS, 5 mM EDTA, 5 mM EGTA, 1 mM sodium orthovanadate, 10 mM sodium pyrophosphate, 10 μM PMSF, 5 μg/ml antipain, 5 μg/ml aprotinin, 5 μg/ml leupeptin). To isolate biotinylated proteins, we used UltraLink-immobilized neutravidin beads (Pierce). After a 2-h incubation, the beads were washed and bound proteins were eluted with SDS sample buffer.

Western immunoblotting

The hippocampal cells were homogenized in ice-cold 0.32 M sucrose containing 0.2 mM sodium orthovanadate, 0.1 mM phenylmethylsulfonyl fluoride, and 5 μg/ml each of antipain, aprotinin, and leupeptin. Protein concentrations were determined by the method of Lowry et al. (1951). Samples were stored at −80 °C until used and were thawed only once. Proteins (20 μg) were solubilized by heating at 100 °C for 5 min in SDS sample buffer (10% glycerol, 5% β-mercaptoethanol, and 2% SDS, in 62.5 mM Tris–HCl, pH 6.8) and were separated on 8 or 12% polyacrylamide gels. Protein blots were reacted with the appropriate antibodies, and the bound antibody was detected by the enhanced chemiluminescence method (Amersham Biosciences Inc., Piscataway, NJ, USA). Quantification of the immunoreactive bands was performed by using an image analyzer (ATTO Co., Tokyo, Japan). Care was taken to ensure that bands

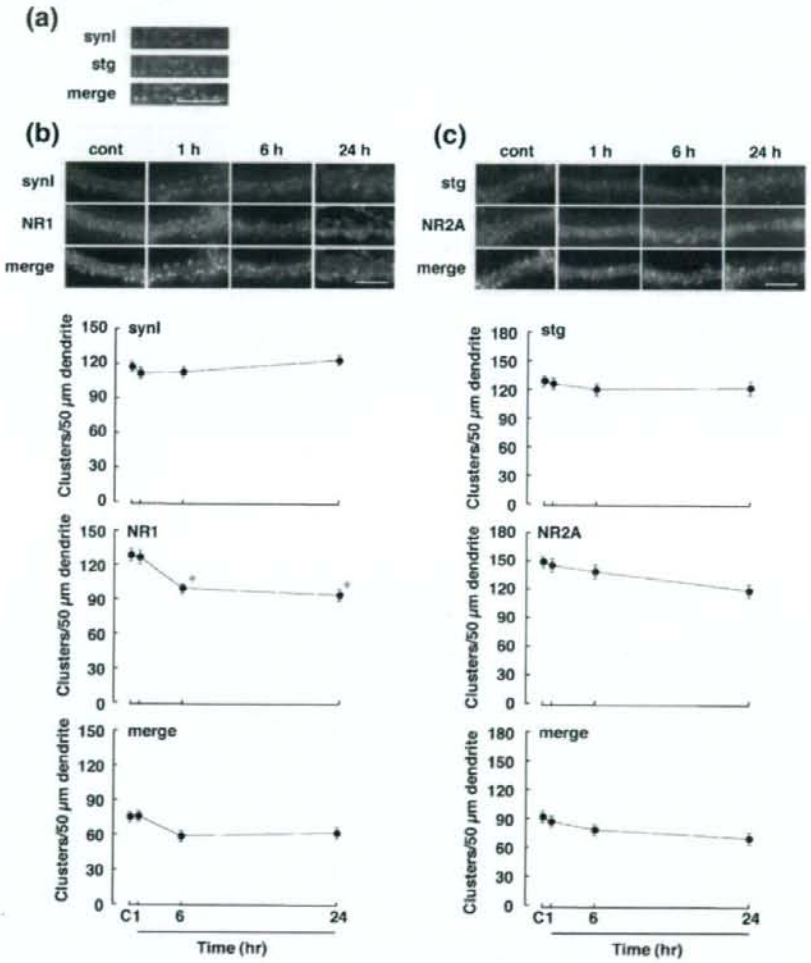

Fig. 2. Time course of changes in the number of clusters including synapsin I and NR1 subunit or synaptotagmin and NR2A subunit after excitotoxicity in cultured hippocampal cells. Hippocampal cells were treated with 100 μM NMDA for 15 min and then incubated in normal conditioned medium without NMDA for 1, 6 or 24 h. (a) Cells were double-immunostained with anti-synapsin I (synI, red) and anti-synaptotagmin (stg, green) antibodies. (b) Hippocampal cells were double-immunostained with anti-synapsin I (synI, red) and anti-NR1 (NR1, green) antibodies. (c) Hippocampal cells were double-immunostained with anti-synaptotagmin (stg, red) and anti-NR2A (NR2A, green) antibodies. Images show magnified regions of dendritic segments. Scale bar, 10 μm. The numbers of clusters positive for synapsin I, NR1, synaptotagmin or NR2A, and those double-positive for synapsin/NR1 or synaptotagmin/NR2A (merged clusters) were counted in a 50-μm dendrite length. Results are expressed as the means ± SEM. *Significant difference from the control group (post hoc Dunnet's *t*-test, $p<0.05$).

to be semiquantified were in the linear range of response. To remove bound antibodies, we incubated the blots for 30 min at 65 °C in 62.5 mM Tris–HCl buffer, pH 6.8, containing 2% SDS and 0.1 M β-mercaptoethanol. The efficiency of the stripping procedure was confirmed by reacting the stripped blot with secondary antibody alone to ensure that no bound antibodies remained.

Antibodies used for immunoblotting were anti-actin (Sigma-Aldrich), anti-NR1 (BD Biosciences, San Jose, CA), anti-NR2A (Upstate Biotechnology, Inc., Lake Placid, NY), anti-NR2B (BD Biosciences), anti-PSD-95 (Affinity BioReagents), anti-CREB (Cell Signaling Technology), and anti-phospho-CREB (Cell Signaling Technology) antibodies.

Silver staining was performed by using a SilverSNAP Stain Kit II (PIERCE, Rockford, IL). After electrophoresis, the gel slab was fixed in 30% ethanol: 10% acetic acid in water for 30 min. It was washed for 10 min with 10% ethanol in water and then for 10 min with water. The gel was sensitized by incubation for 1 min in the SilverSNAP Sensitizer (SilverSNAP Stain Kit II) and it was washed with water. The gel was incubated in Stain Working Solution (SilverSNAP Stain Kit II) and then developed in Developer Working Solution (SilverSNAP Stain Kit II). When the desired intensity of staining was achieved, the development was terminated with 5% acetic acid.

Statistics

The results were expressed as the means ± SEM. Statistical comparison among multiple groups was evaluated by ANOVA followed by post hoc Dunnet's *t*-test or Fisher's protected least significant difference (PLSD) test. Differences with a probability of 5% or less were considered to be significant ($p<0.05$).

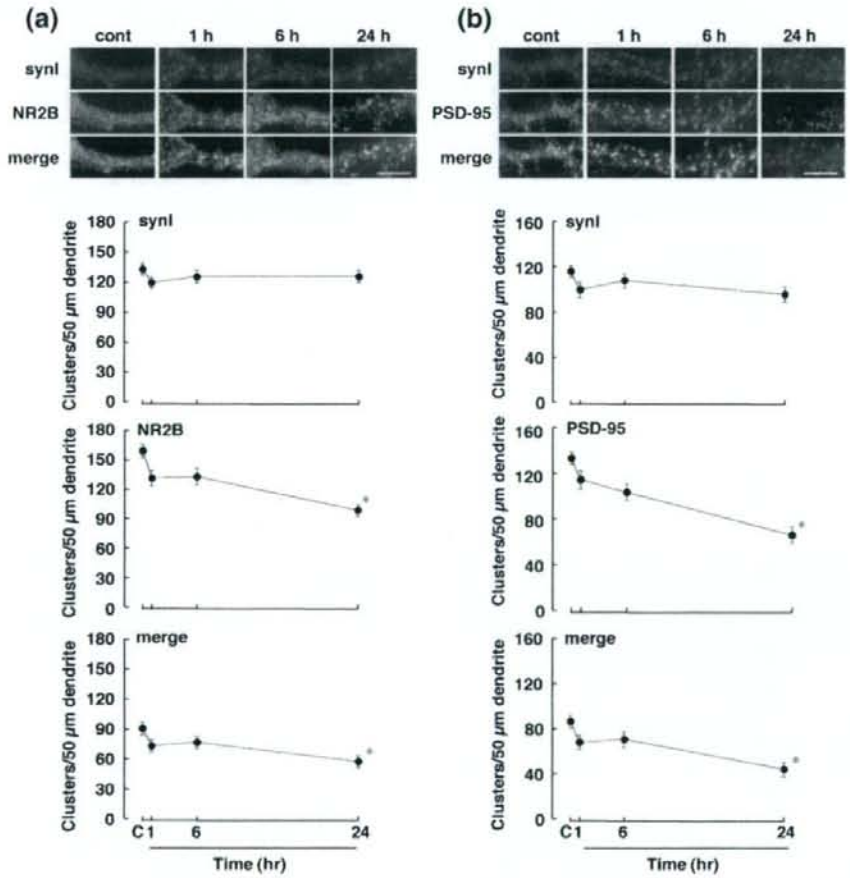

Fig. 3. Time course of changes in the number of clusters including synapsin I and NR2B subunit or synapsin I and PSD-95 after addition of excitotoxic NMDA to cultured hippocampal cells. Hippocampal cells were treated with 100 μM NMDA for 15 min, which treatment was followed by incubation in normal conditioned medium without NMDA for 1, 6 or 24 h. (a) Hippocampal cells were double-immunostained with anti-synapsin I (synI, red) and anti-NR2B (NR2B, green) antibodies. (b) Hippocampal cells were double-immunostained with anti-synapsin I (synI, red) and anti-PSD-95 (PSD-95, green) antibodies. Images show magnified regions of dendritic segments. Scale bar, 10 μm. The numbers of clusters positive for synapsin I, NR2B or PSD-95, and double-positive for synapsin/NR2B or PSD-95 (merged clusters) were counted in a 50-μm dendrite length. Results are expressed as the means ± SEM. *Significant difference from the control group (post hoc Dunnet's *t*-test, $p<0.05$).

Results

First, we examined the effects of HGF on NMDA-induced neuronal cell damage. The concentrations of NMDA (100 μM) and HGF (30 ng/ml) used in the present study were based on data obtained in our previous study (Ishihara et al., 2005). The number of PI-labeled neurons increased after the application of NMDA without a change in the total number of neurons (Fig. 1a and b). Treatment with HGF attenuated the increase in the number of PI-labeled cells (Fig. 1c) without changing the total number of neurons 24 h after the application of NMDA (Fig. 1d).

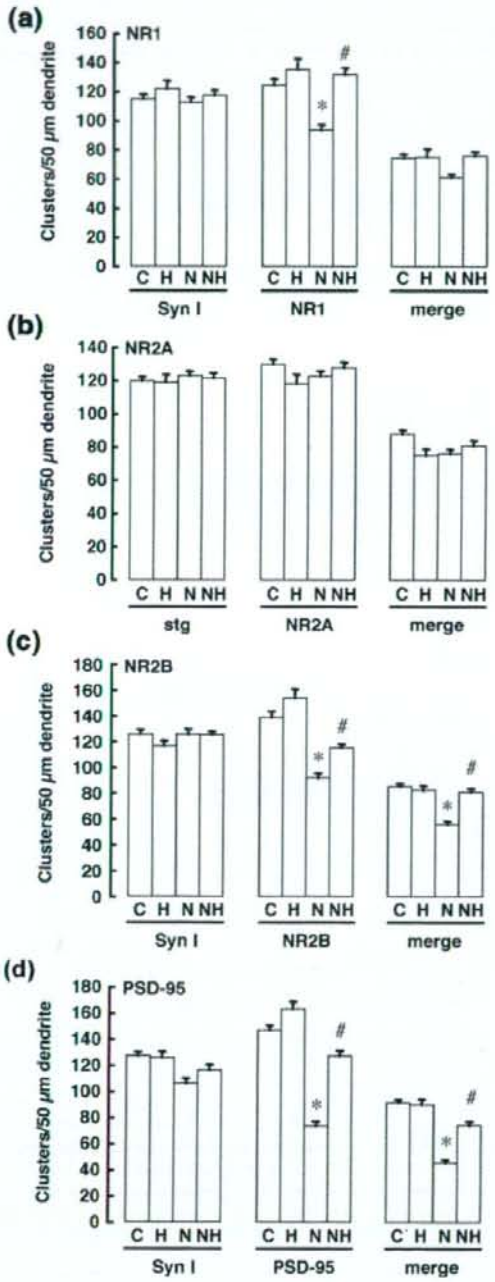

Next, the effects of excitotoxicity on clustering and synaptic localization of the NMDA receptor and PSD-95 were examined. Exposure of cultured hippocampal cells to 100 μM NMDA decreased the number of NR1 clusters starting from 6 h after NMDA addition without changing the number of synapsin I, a presynaptic marker protein, -positive puncta (Fig. 2b). Although NR1 clusters were decreased in number, the number of double-positive immunofluorescent puncta containing NR1 subunits and synapsin was not altered (Fig. 2b). We next explored the time course of changes in the number of clusters of NR2 subunits. In the present study, we could not obtain commercially available mouse anti-NR2A antibodies and attempts to examine immunostaining of synapsin I using mouse anti-synapsin I antibody were not successful. Therefore, we decided to examine double immunostaining of NR2A and synaptotagmin, as a presynaptic marker. At first, we identified the localization of different proteins, synapsin I and synaptotagmin. Double immunostaining of synapsin I and synaptotagmin revealed a high degree of cluster colocalization (Fig. 2a). Therefore, the results indicate evidence about the similarity of localization of synapsin I and synaptotagmin. The density of neither NR2A subunits nor synaptotagmin was altered throughout the experiment (Fig. 2c). In contrast, the number of NR2B clusters was decreased at 24 h after the exposure to 100 μM NMDA for 15 min without a change in the number of synapsin clusters (Fig. 3a). The number of NR2B clusters colocalized with synapsin was also decreased at 24 h after the application of NMDA (Fig. 3a). In addition to NMDA receptor subunits, we investigated the number of clusters positive for PSD-95, which is a receptor-anchoring protein. Their number dropped as did the number of double-positive immunofluorescent puncta containing PSD-95 and synapsin at 24 h after the application of NMDA for 15 min (Fig. 3b).

Since the composition of NMDA receptor complex containing PSD-95 at postsynaptic sites would be altered at 24 h after the excitotoxicity, we next examined the effects of HGF on the number of clusters at 24 h after the application of 100 μM NMDA for 15 min. As shown in Fig. 4, treatment with HGF attenuated the decrease in the number of NR1 clusters without changing the number of synapsin clusters or double-positive immunofluorescent puncta (Fig. 4a). Whereas treatment with

Fig. 4. Effects of HGF on the number of clusters after excitotoxicity in cultured hippocampal cells. Cultured hippocampal cells were incubated with (NH) or without (N) 30 ng/ml HGF for 1 h before the addition of 100 μM NMDA. "H" indicates HGF treatment without excitotoxicity. "C" indicates the incubation under normal culture conditions for 24 h without NMDA treatment. Then, the cells were incubated in normal conditioned medium without NMDA for 24 h and double-immunostained with the indicated antibodies. The numbers of clusters containing synapsin I and NR1 (a), synaptotagmin and NR2A (b), synapsin I and NR2B (c) or synapsin I and PSD-95 (d) were counted in a 50-μm dendrite length. Results are expressed as the means ± SEM. *Significant difference from the control group (post hoc Fisher's PLSD, $p<0.05$). #Significant difference from the NMDA-treated group (post hoc Fisher's PLSD, $p<0.05$).

HGF had no effect on the number of NR2A clusters (Fig. 4b), the decrease in the number of NR2B (Fig. 4c) or PSD-95 (Fig. 4d) clusters was attenuated with HGF treatment without a change in the number of synapsin clusters. Treatment with HGF also lessened the decrease in the number of double-positive immunofluorescent puncta containing NR2B and synapsin (Fig. 4c) or PSD-95 and synapsin (Fig. 4d). Treatment with HGF had no effect on the number of clusters under non-excitotoxic conditions (Fig. 4).

We next focused on the surface expression of the NMDA receptor. To assess this, we performed a cell-surface biotinylation assay using cultured hippocampal cells. First, we confirmed that actin was not contained in the biotinylated proteins after the application of NMDA for 15 min (Fig. 5a). The protein composition of biotinylated samples under excitotoxic conditions was comparable to that under normal conditions throughout the experiment (Fig. 5b and c). As shown in Fig. 5d, the surface expression of NR1 subunit was not altered under excitotoxic conditions. Conversely, the amounts of NR2A and NR2B subunits at the cell surface were significantly decreased starting 1 h after the application of NMDA, and the decreased levels were maintained throughout the experiment (Fig. 5e and f).

We next determined the effects of HGF on the surface expression of NMDA receptor subunits. After the application of NMDA for 15 min, the cells were incubated in normal conditioned medium without NMDA for 24 h. Biotinylated proteins

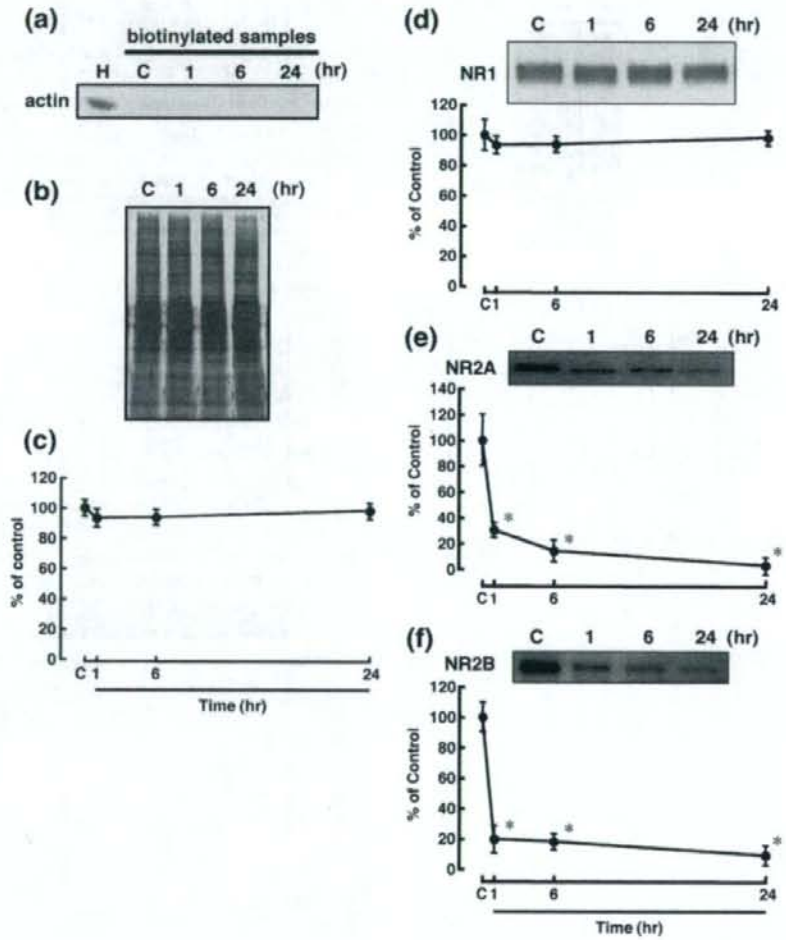

Fig. 5. Time course of changes in the levels of proteins at the cell surface after excitotoxicity in cultured hippocampal cells. Hippocampal cells were treated with NMDA for 15 min and then incubated in normal conditioned medium without NMDA for 1, 6 or 24 h. Thereafter, proteins at the cell surface were labeled with membrane-impermeable sulfo-NHS-SS-biotin, which labeling was followed by precipitation with UltraLink-immobilized neutravidin beads. (a) Biotinylated proteins were probed with anti-actin antibody to confirm that actin was not present in the biotinylated samples. "H" indicates total brain homogenate. (b) Total protein composition of biotinylated samples was determined by silver staining. (c) The gel in silver staining was scanned. Total protein composition was not changed throughout the experiment. Results are expressed as the mean percentages of control ± SEM. (d, e, and f) Biotinylated proteins were immunoblotted with anti-NR1 (d), anti-NR2A (e), and anti-NR2B (f) antibodies. Bands corresponding to NR1, NR2A, and NR2B were scanned. Results are expressed as the mean percentages of control ± SEM. *Significant difference from the control group (post hoc Dunnet's t-test, $p<0.05$).

were not reactive with the antibody against actin regardless of treatment or not with HGF (Fig. 6a). The protein composition of biotinylated samples was unaffected irrespective of HGF treatment (Fig. 6b and c). HGF treatment did not alter the surface expression of NR1 subunit throughout the experiment (Fig. 6d). The decrease in NR2B subunit density at the surface was

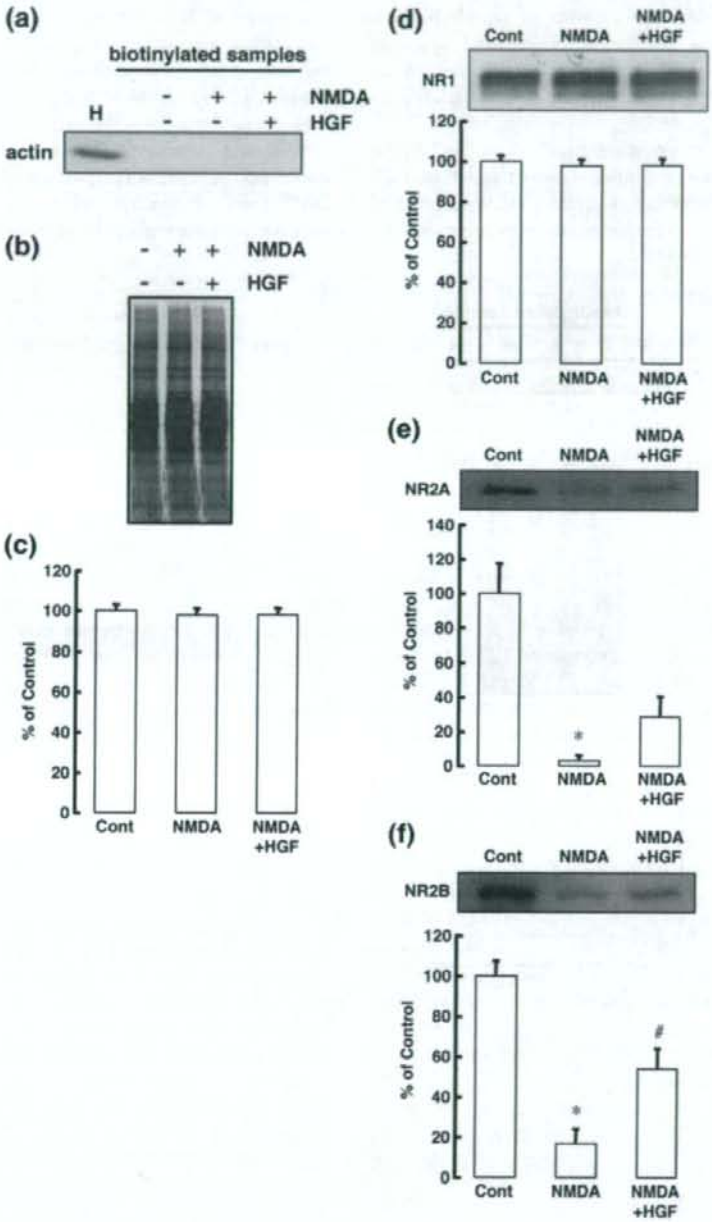

Fig. 6. Effects of HGF on the levels of proteins at the cell surface after excitotoxicity in cultured hippocampal cells. Hippocampal cells were treated with or without HGF for 1 h before the addition of NMDA for 15 min. Then, the cells were incubated in normal conditioned medium without NMDA for 24 h. Proteins at the cell surface were labeled with membrane-impermeable sulfo-NHS-SS-biotin and then precipitated with UltraLink-immobilized neutravidin beads. (a) Biotinylated proteins were probed with anti-actin antibody to confirm that actin was not present in the biotinylated samples. "H" indicates total brain homogenate. (b) Total protein composition of biotinylated samples was determined by silver staining. (c) The gel in silver staining was scanned. Total protein composition was not changed throughout the experiment. Results are expressed as the mean percentages of the control ± SEM. (d, e, and f) Biotinylated proteins were immunoblotted with anti-NR1 (d), anti-NR2A (e), and anti-NR2B (f) antibodies. Bands corresponding to NR1, NR2A, and NR2B were scanned. Results are expressed as the mean percentages of the control ± SEM. *Significant difference from the control group (post hoc Fisher's PLSD, $p<0.05$). #Significant difference from the NMDA-treated group (post hoc Fisher's PLSD, $p<0.05$).

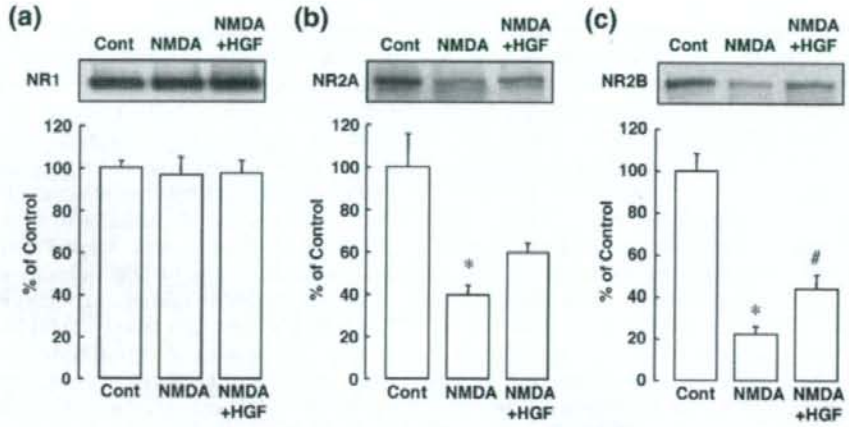

Fig. 7. Effects of HGF on the levels of proteins at the cell surface after excitotoxicity in cultured hippocampal cells. Hippocampal cells were treated with or without HGF for 1 h before the addition of NMDA for 15 min. Then, the cells were incubated in normal conditioned medium without NMDA for 1 h. Proteins at the cell surface were labeled with membrane-impermeable sulfo-NHS-SS-biotin and then precipitated with UltraLink-immobilized neutravidin beads. Biotinylated proteins were immunoblotted with anti-NR1 (a), anti-NR2A (b), and anti-NR2B (c) antibodies. Bands corresponding to NR1, NR2A, and NR2B were scanned. Results are expressed as the mean percentages of the control ± SEM. *Significant difference from the control group (post hoc Fisher's PLSD, $p<0.05$). #Significant difference from the NMDA-treated group (post hoc Fisher's PLSD, $p<0.05$).

inhibited and that in NR2A tended to be attenuated by the HGF treatment (Fig. 6e and f).

We next examined the effects of HGF on the surface expression of NMDA receptor subunits at the early stage. Surface-biotinylated proteins were isolated at 1 h after the application of NMDA. The surface expression of NR1 subunit was not altered regardless of treatment or not with HGF compared with that of control group (Fig. 7a). The decrease in the amounts of NR2B (Fig. 7c) subunits at the cell surface was inhibited and that in NR2A (Fig. 7b) tended to be attenuated by the HGF treatment.

As it is known that stimulation of NMDA receptors of hippocampal neurons induces phosphorylation of CREB, we next examined the effect of HGF on high K^+-stimulated CREB phosphorylation at 24 h after the application of NMDA. Cultured hippocampal cells were pretreated with 10 μM CNQX, 10 μM nifedipine, and 0.3 μM TTX to suppress spontaneous activity. First, we found that basal phosphorylation of CREB was not altered by treatment with 10 μM MK-801 (Fig. 8a). Stimulation with 60 mM KCl induced phosphorylation of CREB, and MK-801 inhibited CREB phosphorylation (Fig. 8b). Under this condition, high K^+-stimulated phosphorylation of CREB was significantly decreased at 24 h after the application of NMDA (Fig. 8c). Treatment with HGF attenuated the decrease in CREB phosphorylation induced by high K^+-stimulation (Fig. 8c).

Discussion

We previously demonstrated that treatment with HGF decreased neuronal death in the *in vivo* ischemic brain (Date et al., 2004; Niimura et al., 2006). Furthermore, in cultured hippocampal neurons, HGF exerted protective effects by acting directly on neurons under the excitotoxic condition (Ishihara et al., 2005). In accordance with this, the protective effects of HGF against neurotoxicity in the present study were comparable to those found in that previous study. Although these effects of HGF may contribute to prevention from learning and memory dysfunction seen after cerebral ischemia (Date et al., 2004), it is still not clear whether synapses under the excitotoxic condition were morphologically and functionally improved by treatment with HGF. So we investigated the effects of HGF on synaptic clustering of the NMDA receptor and PSD-95, and on the biochemical response to excitatory input through the NMDA receptor after the excitotoxic injury.

In control hippocampal cultures, the presynaptic marker proteins synapsin and synaptotagmin were localized at dendritic puncta; and approximately 60% of dendritic clustered NMDA receptor subunits NR1, NR2A, and NR2B were colocalized with these presynaptic marker proteins. Whereas the number of synapsin or synaptotagmin clusters was not altered under the excitotoxic condition, that of NR1 clusters was decreased. Although the limited resolution of fluorescent measurements might preclude identification of smaller individual puncta, the finding that the number of double-positive immunofluorescent puncta containing NR1 subunit and synapsin was not altered suggests that mainly the extrasynaptic NR1 subunits might be decreased in number. The synaptic localization of NR2B was decreased at 24 h after the excitotoxic injury, although the number of synaptic NR2A clusters was not altered throughout the experiment. These results suggest that NR2A subunit would have remained in the NMDA receptor complex at synapses under the excitotoxic condition. Earlier it was shown that cell death mediated by the NMDA receptor was greater in transfected HEK293 cells expressing NR1/NR2A receptors than NR1/NR2B receptors (Anegawa et al., 1995). In addition, the infarct volume after focal ischemia was decreased in mice lacking the NR2A subunit (Morikawa et al., 1998), suggesting that the NR2A subunit plays a key role in neuronal injuries. However,

roles of NR2A subunit in pathological conditions remain unclear and controversial, since the surface expression of NR2A subunits was decreased after excitotoxic injury in the present study. In contrast to NR2A subunit, it is conceivable that NR2B subunits disappeared from synapses. Mutant mice defective in the NR2B subunit showed a failure of neuronal pattern formation and synaptic plasticity (Kutsuwada et al., 1996). Conversely, overexpression of NMDA receptor subunit NR2B in the forebrain of mice resulted in superior ability in learning and memory function in behavioral tasks (Tang et al., 1999). Therefore, the decreased number of NR2B clusters implies the dysfunction of the NMDA receptor. However, a contribution of NR2A subunit to exert physiological function cannot be fully ruled out, since disruption of the NR2A subunit gene reduces the NMDA receptor channel current and results in a deficiency in spatial learning (Sakimura et al., 1995). We also demonstrated that synaptic localization of PSD-95 was decreased at 24 h. In the postsynaptic density, the binding of PSD-95 to NR2 subunits has been implicated in the localization and anchoring of receptors and signaling proteins to the postsynaptic density, and in the regulation of ion-channel function, synaptic activity, and intracellular signaling (Kim and Sheng, 2004; Migaud et al., 1998; Sattler et al., 1999; Yamada et al., 1999). For example, PSD-95-mutant mice showed alteration of synaptic plasticity and failure of spatial learning (Migaud et al., 1998). A marked decrease in the levels of NR2 subunits and PSD-95 would indicate that levels of functional receptors might be decreased. This was consistent with failure of CREB phosphorylation in response to depolarization-evoked NMDA receptor activation in the present study. Therefore, the disturbance of appropriate clustering of NMDA receptors and PSD-95 at synapses may lead to dysfunction of glutamatergic neurotransmission, which ultimately causes impairment of learning and memory function.

In the present study, HGF attenuated the decreased synaptic localization of NR2B and PSD-95. Functional localization of the NMDA receptor at synapses depends on PSD-95 (Barria and Malinow, 2002; Mori et al., 1998; Prybylowski et al., 2002; Steigerwald et al., 2000). Recently, we demonstrated that HGF increased the number of puncta of PSD-95 in young hippocampal neuron (Nakano et al., 2007). These findings suggest that HGF might modulate the synaptic expression of the NMDA receptor by regulating the localization of PSD-95. Interestingly, tyrosine-phosphorylated NMDA receptors induced by tyrosine kinase Src were not truncated by calpain (Rong et al., 2001). PKC, which is one of the upstream components of Src activation (Lu et al., 1999; Macdonald et al., 2005), can be activated by HGF in neurons (Machide et al., 1998). Therefore, the results in the present study suggest the possibility that HGF may prevent the degradation of NMDA receptor subunits through

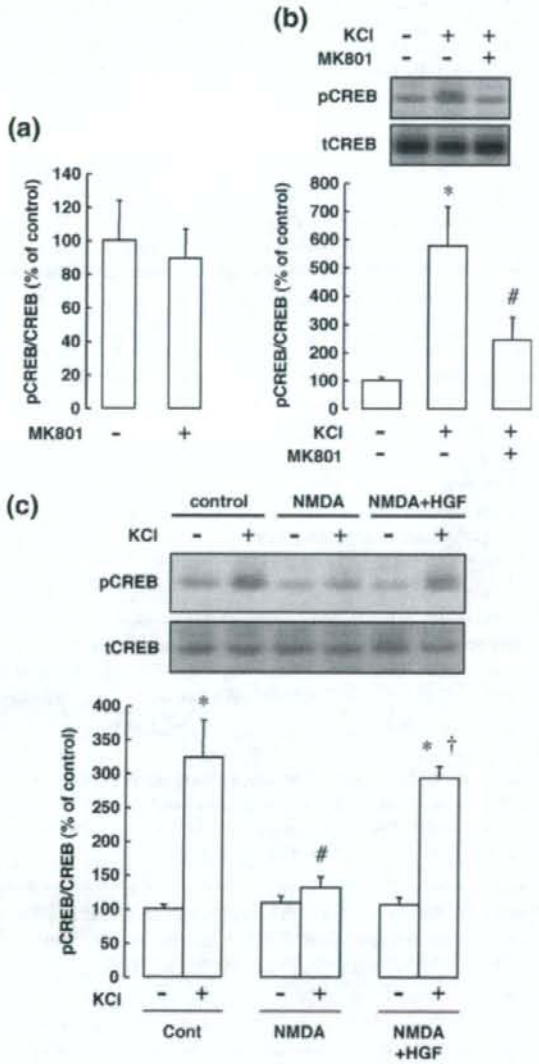

Fig. 8. Effects of HGF on NMDA receptor-mediated CREB phosphorylation after excitotoxicity in cultured hippocampal cells. (a) Cultured hippocampal cells were pretreated with 10 μM CNQX, 10 μM nifedipine, and 0.3 μM TTX for 30 min and then incubated for 3 min with or without 10 μM MK-801. Total cell lysates were probed with anti-phospho CREB (pCREB) and anti-total CREB (tCREB) antibodies. Bands corresponding to pCREB were scanned, and the scanned bands were normalized by tCREB on the same blot. (b) Cultured hippocampal cells were pretreated with 10 μM CNQX, 10 μM nifedipine, and 0.3 μM TTX for 30 min, which pretreatment was followed by stimulation with 60 mM KCl for 3 min with or without 10 μM MK-801. Total cell lysates were probed with anti-phospho CREB (pCREB) and anti-total CREB (tCREB) antibodies. Results are expressed as the mean percentages of control±SEM. *Significant difference from the untreated group (post hoc Fisher's PLSD, $p<0.05$). #Significant difference from the high-K^+-stimulation group (post hoc Fisher's PLSD, $p<0.05$). (c) Cultured hippocampal cells were pretreated or not with HGF for 1 h before the addition of NMDA for 15 min. Then, the cells were incubated in normal conditioned medium without NMDA for 24 h. Thereafter the cells were incubated with 10 μM CNQX, 10 μM nifedipine, and 0.3 μM TTX for 30 min and subsequently stimulated or not with 60 mM KCl for 3 min. Total cell lysates were probed with anti-phospho CREB (pCREB) and anti-total CREB (tCREB) antibodies. Results are expressed as the mean percentages of the control±SEM. *Significant difference from the high-K^+-untreated group (post hoc Fisher's PLSD, $p<0.05$). #Significant difference from the high-K^+-stimulated control group (post hoc Fisher's PLSD, $p<0.05$). †Significant difference from the high-K^+-stimulated NMDA-treated group (post hoc Fisher's PLSD, $p<0.05$).

promoting protein phosphorylation. Synaptic structures are not homogenously distributed along a dendrite and are an important determinant of its function. It will be important to determine whether the pathophysiological changes are dependent of the order of dendrites or restricted to apical or basal dendrites.

We further demonstrated that the surface expression of the NMDA receptor subunits NR2A and NR2B, which modulate the properties of heteromeric NR1/NR2 receptors, was decreased by excitotoxicity. In the present study, there was an inconsistency between the number of clusters of NMDA receptor subunits and the surface expression of receptor subunits. A possible reason is suggested to be that the expression of NR2 subunits on cell surfaces is vulnerable to excitotoxic stimulation. On the other hand, the surface expression of NR1 subunit was not altered throughout the experiment, although NR1 clusters were decreased in number. Although immunolabeled puncta on dendritic segments might include intracellular and/or extrasynaptic receptors, our results are consistent with the findings that NR2 subunit is rapidly cleaved after NMDA receptor stimulation with no cleavage of NR1 (Simpkins et al., 2003) and that NR1 immunoreactivity in the cell-surface fraction was not changed after application of glutamate (Wu et al., 2007). We demonstrated that the decreased amounts of NMDA receptor subunits at the cell surface were attenuated by treatment with HGF. This might be due to the protective effect of HGF against neuronal cell death at 24 h after the application of NMDA. In the present study, surface expression of NR2 subunits was significantly decreased at the early period after excitotoxicity. Therefore, we next assessed effects of HGF on the surface expression of NMDA receptor subunits at 1 h after the application of NMDA, when cell death did not occur. We demonstrated that the decrease in surface expression of NR2 subunits tended to be inhibited by HGF treatment. The results suggest that HGF has the ability to attenuate decreases in the NMDA receptor at the cell surface under excitotoxic conditions. The decreases in the surface expression of NR2 subunits may result in a disturbance of intracellular signaling pathways through the NMDA receptor. The prevention of ischemia-induced learning and memory dysfunction by HGF treatment as observed in a previous study (Date et al., 2004) might contribute to the improvement of NMDA receptor localization and intracellular signaling.

The next important issue is whether attenuation of the number of clusters and surface localization of NMDA receptor subunits by HGF treatment is related to an improvement of activity-dependent biochemical response. In this sense, failure of CREB phosphorylation in response to depolarization-evoked NMDA receptor activation was attenuated by HGF treatment. It has been well characterized that CREB is involved in the acquisition of learning and memory (Konradi and Heckers, 2003). Although it is conceivable that CREB phosphorylation in cultured cells is a marker of NMDA receptor signaling and learning and memory function, the results in the present study suggest that HGF improved the ability of intracellular signaling components to phosphorylate CREB via the NMDA receptor.

Whereas the NMDA receptor plays a pivotal role in physiological activities in the central nervous system such as learning and memory function, the excessive activation of the receptor is involved in a variety of neurological and neurodegenerative disorders. Therefore, it is important to explore strategies to protect brain cells from NMDA receptor-mediated injury under pathophysiological conditions. The present findings suggest that treatment with HGF is capable of improving not only synaptic localization of NMDA receptor subunits but also physiological intracellular signaling via the NMDA receptor.

Acknowledgment

This work was supported by the Promotion and Mutual Aid Corporation for Private Schools of Japan.

References

Achim, C.L., Katyal, S., Wiley, C.A., Shiratori, M., Wang, G., Oshika, E., Petersen, B.E., Li, J.M., Michalopoulos, G.K., 1997. Expression of HGF and cMet in the developing and adult brain. Brain Res. Dev. Brain Res. 102, 299–303.

Anegawa, N.J., Lynch, D.R., Verdoorn, T.A., Pritchett, D.B., 1995. Transfection of *N*-methyl-D-aspartate receptors in a nonneuronal cell line leads to cell death. J. Neurochem. 64, 2004–2012.

Balkovetz, D.F., Lipschutz, J.H., 1999. Hepatocyte growth factor and the kidney: it is not just for the liver. Int. Rev. Cytol. 186, 225–260.

Barria, A., Malinow, R., 2002. Subunit-specific NMDA receptor trafficking to synapses. Neuron 35, 345–353.

Brenman, J.E., Chao, D.S., Gee, S.H., McGee, A.W., Craven, S.E., Santillano, D.R., Wu, Z., Huang, F., Xia, H., Peters, M.F., Froehner, S.C., Bredt, D.S., 1996. Interaction of nitric oxide synthase with the postsynaptic density protein PSD-95 and alpha1-syntrophin mediated by PDZ domains. Cell 84, 757–767.

Chen, H.J., Rojas-Soto, M., Oguni, A., Kennedy, M.B., 1998. A synaptic Ras-GTPase activating protein (p135 SynGAP) inhibited by CaM kinase II. Neuron 20, 895–904.

Cho, K.O., Hunt, C.A., Kennedy, M.B., 1992. The rat brain postsynaptic density fraction contains a homolog of the Drosophila discs-large tumor suppressor protein. Neuron 9, 929–942.

Dale, N., Roberts, A., 1985. Dual-component amino-acid-mediated synaptic potentials: excitatory drive for swimming in *Xenopus* embryos. J. Physiol. 363, 35–59.

Das, S., Sasaki, Y.F., Rothe, T., Premkumar, L.S., Takasu, M., Crandall, J.E., Dikkes, P., Conner, D.A., Rayudu, P.V., Cheung, W., Chen, H.S., Lipton, S.A., Nakanishi, N., 1998. Increased NMDA current and spine density in mice lacking the NMDA receptor subunit NR3A. Nature 393, 377–381.

Date, I., Takagi, N., Takagi, K., Kago, T., Matsumoto, K., Nakamura, T., Takeo, S., 2004. Hepatocyte growth factor improved learning and memory dysfunction of microsphere-embolized rats. J. Neurosci. Res. 78, 442–453.

Dingledine, R., Borges, K., Bowie, D., Traynelis, S.F., 1999. The glutamate receptor ion channels. Pharmacol. Rev. 51, 7–61.

Hamanoue, M., Takemoto, N., Matsumoto, K., Nakamura, T., Nakajima, K., Kohsaka, S., 1996. Neurotrophic effect of hepatocyte growth factor on central nervous system neurons in vitro. J Neurosci. Res. 43, 554–564.

Hollmann, M., Heinemann, S., 1994. Cloned glutamate receptors. Annu. Rev. Neurosci. 17, 31–108.

Honda, S., Kagoshima, M., Wanaka, A., Tohyama, M., Matsumoto, K., Nakamura, T., 1995. Localization and functional coupling of HGF and c-Met/HGF receptor in rat brain: implication as neurotrophic factor. Brain Res. Mol. Brain Res. 32, 197–210.

Huettner, J.E., Baughman, R.W., 1986. Primary culture of identified neurons from the visual cortex of postnatal rats. J. Neurosci. 6, 3044–3060.

Ishihara, N., Takagi, N., Niimura, M., Takagi, K., Nakano, M., Tanonaka, K., Funakoshi, H., Matsumoto, K., Nakamura, T., Takeo, S., 2005. Inhibition of apoptosis-inducing factor translocation is involved in protective effects of hepatocyte growth factor against excitotoxic cell death in cultured hippocampal neurons. J. Neurochem. 95, 1277–1286.

Ishii, T., Moriyoshi, K., Sugihara, H., Sakurada, K., Kadotani, H., Yokoi, M., Akazawa, C., Shigemoto, R., Mizuno, N., Masu, M., et al., 1993. Molecular characterization of the family of the *N*-methyl-D-aspartate receptor subunits. J. Biol. Chem. 268, 2836–2843.

Kennedy, M.B., 1997. The postsynaptic density at glutamatergic synapses. Trends Neurosci. 20, 264–268.

Kim, E., Sheng, M., 2004. PDZ domain proteins of synapses. Nat. Rev. Neurosci. 5, 771–781.

Kim, J.H., Liao, D., Lau, L.F., Huganir, R.L., 1998. SynGAP: a synaptic RasGAP that associates with the PSD-95/SAP90 protein family. Neuron 20, 683–691.

Klauck, T.M., Scott, J.D., 1995. The postsynaptic density: a subcellular anchor for signal transduction enzymes. Cell Signal 7, 747–757.

Konradi, C., Heckers, S., 2003. Molecular aspects of glutamate dysregulation: implications for schizophrenia and its treatment. Pharmacol. Ther. 97, 153–179.

Kutsuwada, T., Sakimura, K., Manabe, T., Takayama, C., Katakura, N., Kushiya, E., Natsume, R., Watanabe, M., Inoue, Y., Yagi, T., Aizawa, S., Arakawa, M., Takahashi, T., Nakamura, Y., Mori, H., Mishina, M., 1996. Impairment of suckling response, trigeminal neuronal pattern formation, and hippocampal LTD in NMDA receptor epsilon 2 subunit mutant mice. Neuron 16, 333–344.

Lowry, O.H., Rosebrough, N.J., Farr, A.L., Randall, R.J., 1951. Protein measurement with the Folin phenol reagent. J. Biol. Chem. 193, 265–275.

Lu, W.Y., Xiong, Z.G., Lei, S., Orser, B.A., Dudek, E., Browning, M.D., MacDonald, J.F., 1999. G-protein-coupled receptors act via protein kinase C and Src to regulate NMDA receptors. Nat Neurosci 2, 331–338.

Macdonald, D.S., Weerapura, M., Beazely, M.A., Martin, L., Czerwinski, W., Roder, J.C., Orser, B.A., MacDonald, J.F., 2005. Modulation of NMDA receptors by pituitary adenylate cyclase activating peptide in CA1 neurons requires G alpha q, protein kinase C, and activation of Src. J. Neurosci. 25, 11374–11384.

Machide, M., Kamitori, K., Nakamura, Y., Kohsaka, S., 1998. Selective activation of phospholipase C gamma1 and distinct protein kinase C subspecies in intracellular signaling by hepatocyte growth factor/scatter factor in primary cultured rat neocortical cells. J. Neurochem. 71, 592–602.

Matsumoto, K., Nakamura, T., 1996. Emerging multipotent aspects of hepatocyte growth factor. J. Biochem. (Tokyo) 119, 591–600.

Matsumoto, K., Nakamura, T., 2001. Hepatocyte growth factor: renotropic role and potential therapeutics for renal diseases. Kidney Int. 59, 2023–2038.

Migaud, M., Charlesworth, P., Dempster, M., Webster, L.C., Watabe, A.M., Makhinson, M., He, Y., Ramsay, M.F., Morris, R.G., Morrison, J.H., O'Dell, T.J., Grant, S.G., 1998. Enhanced long-term potentiation and impaired learning in mice with mutant postsynaptic density-95 protein. Nature 396, 433–439.

Monyer, H., Sprengel, R., Schoepfer, R., Herb, A., Higuchi, M., Lomeli, H., Burnashev, N., Sakmann, B., Seeburg, P.H., 1992. Heteromeric NMDA receptors: molecular and functional distinction of subtypes. Science 256, 1217–1221.

Mori, H., Manabe, T., Watanabe, M., Satoh, Y., Suzuki, N., Toki, S., Nakamura, K., Yagi, T., Kushiya, E., Takahashi, T., Inoue, Y., Sakimura, K., Mishina, M., 1998. Role of the carboxy-terminal region of the GluR epsilon2 subunit in synaptic localization of the NMDA receptor channel. Neuron 21, 571–580.

Morikawa, E., Mori, H., Kiyama, Y., Mishina, M., Asano, T., Kirino, T., 1998. Attenuation of focal ischemic brain injury in mice deficient in the epsilon1 (NR2A) subunit of NMDA receptor. J. Neurosci. 18, 9727–9732.

Moriyoshi, K., Masu, M., Ishii, T., Shigemoto, R., Mizuno, N., Nakanishi, S., 1991. Molecular cloning and characterization of the rat NMDA receptor. Nature 354, 31–37.

Nakamura, T., Nawa, K., Ichihara, A., 1984. Partial purification and characterization of hepatocyte growth factor from serum of hepatectomized rats. Biochem. Biophys. Res. Commun. 122, 1450–1459.

Nakamura, T., Nishizawa, T., Hagiya, M., Seki, T., Shimonishi, M., Sugimura, A., Tashiro, K., Shimizu, S., 1989. Molecular cloning and expression of human hepatocyte growth factor. Nature 342, 440–443.

Nakanishi, S., 1992. Molecular diversity of glutamate receptors and implications for brain function. Science 258, 597–603.

Nakano, M., Takagi, N., Takagi, K., Funakoshi, H., Matsumoto, K., Nakamura, T., Takeo, S., 2007. Hepatocyte growth factor promotes the number of PSD-95 clusters in young hippocampal neurons. Exp. Neurol.

Niimura, M., Takagi, N., Takagi, K., Mizutani, R., Ishihara, N., Matsumoto, K., Funakoshi, H., Nakamura, T., Takeo, S., 2006. Prevention of apoptosis-inducing factor translocation is a possible mechanism for protective effects of hepatocyte growth factor against neuronal cell death in the hippocampus after transient forebrain ischemia. J. Cereb. Blood Flow Metab. 26, 1354–1365.

Nishi, M., Hinds, H., Lu, H.P., Kawata, M., Hayashi, Y., 2001. Motoneuron-specific expression of NR3B, a novel NMDA-type glutamate receptor subunit that works in a dominant-negative manner. J. Neurosci. 21, RC185.

Prybylowski, K., Fu, Z., Losi, G., Hawkins, L.M., Luo, J., Chang, K., Wenthold, R.J., Vicini, S., 2002. Relationship between availability of NMDA receptor subunits and their expression at the synapse. J. Neurosci. 22, 8902–8910.

Rong, Y., Lu, X., Bernard, A., Khrestchatisky, M., Baudry, M., 2001. Tyrosine phosphorylation of ionotropic glutamate receptors by Fyn or Src differentially modulates their susceptibility to calpain and enhances their binding to spectrin and PSD-95. J. Neurochem. 79, 382–390.

Sakimura, K., Kutsuwada, T., Ito, I., Manabe, T., Takayama, C., Kushiya, E., Yagi, T., Aizawa, S., Inoue, Y., Sugiyama, H., et al., 1995. Reduced hippocampal LTP and spatial learning in mice lacking NMDA receptor epsilon 1 subunit. Nature 373, 151–155.

Sattler, R., Xiong, Z., Lu, W.Y., Hafner, M., MacDonald, J.F., Tymianski, M., 1999. Specific coupling of NMDA receptor activation to nitric oxide neurotoxicity by PSD-95 protein. Science 284, 1845–1848.

Shen, L., Liang, F., Walensky, L.D., Huganir, R.L., 2000. Regulation of AMPA receptor GluR1 subunit surface expression by a 4. 1N-linked actin cytoskeletal association. J. Neurosci. 20, 7932–7940.

Simpkins, K.L., Guttmann, R.P., Dong, Y., Chen, Z., Sokol, S., Neumar, R.W., Lynch, D.R., 2003. Selective activation induced cleavage of the NR2B subunit by calpain. J. Neurosci. 23, 11322–11331.

Steigerwald, F., Schulz, T.W., Schenker, L.T., Kennedy, M.B., Seeburg, P.H., Kohr, G., 2000. C-Terminal truncation of NR2A subunits impairs synaptic but not extrasynaptic localization of NMDA receptors. J. Neurosci. 20, 4573–4581.

Sun, W., Funakoshi, H., Nakamura, T., 2002a. Localization and functional role of hepatocyte growth factor (HGF) and its receptor c-met in the rat developing cerebral cortex. Brain Res. Mol. Brain Res. 103, 36–48.

Sun, W., Funakoshi, H., Nakamura, T., 2002b. Overexpression of HGF retards disease progression and prolongs life span in a transgenic mouse model of ALS. J. Neurosci. 22, 6537–6548.

Tang, Y.P., Shimizu, E., Dube, G.R., Rampon, C., Kerchner, G.A., Zhuo, M., Liu, G., Tsien, J.Z., 1999. Genetic enhancement of learning and memory in mice. Nature 401, 63–69.

Thompson, J., Dolcet, X., Hilton, M., Tolcos, M., Davies, A.M., 2004. HGF promotes survival and growth of maturing sympathetic neurons by PI-3 kinase- and MAP kinase-dependent mechanisms. Mol. Cell. Neurosci. 27, 441–452.

Wu, H.Y., Hsu, F.C., Gleichman, A.J., Baconguis, I., Coulter, D.A., Lynch, D.R., 2007. Fyn-mediated phosphorylation of NR2B Tyr-1336 controls calpain-mediated NR2B cleavage in neurons and heterologous systems. J. Biol. Chem. 282, 20075–20087.

Yamada, Y., Chochi, Y., Takamiya, K., Sobue, K., Inui, M., 1999. Modulation of the channel activity of the epsilon2/zeta1-subtype *N*-methyl D-aspartate receptor by PSD-95. J. Biol. Chem. 274, 6647–6652.

Zarnegar, R., Michalopoulos, G.K., 1995. The many faces of hepatocyte growth factor: from hepatopoiesis to hematopoiesis. J, Cell. Biol. 129, 1177–1180.

Ziff, E.B., 1997. Enlightening the postsynaptic density. Neuron 19, 1163–1174.

J Neuropathol Exp Neurol

Vol. 68, No. 1
January 2009
pp. 37–47

ORIGINAL ARTICLE

Nuclear TAR DNA Binding Protein 43 Expression in Spinal Cord Neurons Correlates With the Clinical Course in Amyotrophic Lateral Sclerosis

Hisae Sumi, MD, PhD, Shinsuke Kato, MD, PhD, Yuko Mochimaru, Harutoshi Fujimura, MD, PhD, Masaki Etoh, MD, PhD, and Saburo Sakoda, MD, PhD

Abstract

TAR DNA binding protein 43 (TDP-43) has been considered a signature protein in frontotemporal dementia and amyotrophic lateral sclerosis (ALS), but not in ALS associated with the superoxide dismutase 1 (*SOD1*) gene mutations (ALS1). To clarify how TDP may be involved in ALS pathogenesis, clinical and pathological features in cases of sporadic ALS ([SALS] n = 18) and ALS1 (n = 6) were analyzed. In SALS patients with rapid clinical courses, TDP mislocalization (i.e. cytoplasmic staining and TDP-positive cytoplasmic inclusions) in anterior horn cells was frequent. In SALS patients with slow clinical courses, TDP-43 mislocalization was rare. In an ALS1 patient with the *SOD1* gene mutation C111Y, there were numerous TDP-positive inclusions and colocalization of SOD1 and TDP. In mutant SOD1 transgenic (G93A) mice at the end stage (median, 256 days), TDP-positive inclusions and TDP colocalization with SOD1 were also observed; nuclear TDP-43 immunoreactivity was highly correlated with life span in these mice. In both humans and mice, nuclei that stained strongly for TDP were large and circular; weakly stained nuclei were atrophic or deformed. In conclusion, low levels of TDP expression in the nucleus cor relate with a rapid clinical course in SALS and in ALS1 model mice, suggesting that nuclear TDP may play a protective role against motor neuron death resulting from different underlying etiologies.

Key Words: Amyotrophic lateral sclerosis, ALS, Anterior horn cell, ALS1, G93A transgenic mice, Lewy body–like hyaline inclusion, SOD1, TDP-43.

INTRODUCTION

Amyotrophic lateral sclerosis (ALS) is a fatal motor neuron disease that causes progressive motor paralysis. The underlying pathogenetic mechanisms are largely unknown in 90% of ALS patients, that is, those with sporadic ALS (SALS). Of the 10% of ALS cases with familial ALS (FALS), approximately one fifth are associated with a mutation in the superoxide dismutase 1 (*SOD1*) gene; these patients are classified as ALS1 (1, 2). The pathogenesis of ALS1 is thought to involve aggregation of mutant SOD1 and subsequent oxidative stress (3). Another rare cause of juvenile autosomal recessive FALS is the gene that encodes ALS2, also known as alsin (4, 5). In most cases of FALS, however, the causative gene has not been identified because of low penetrance.

TAR DNA binding protein 43 (TDP-43), a nuclear protein, contains 2 fully functional RNA recognition motif domains and a C-terminal region that is capable of binding directly to several proteins of the heterogeneous nuclear ribonucleoprotein family (6–8); these ribonucleoproteins have a variety of functions including the modification, stabilization, and transport of RNA. The TDP modifies the splicing of exon 9 of the cystic fibrosis transmembrane conductance regulator gene (9) and of exon 3 of the apolipoprotein A-II gene (10). Recently, it also has been reported that loss of TDP in vitro results in nuclear dysmorphism, misregulation of the cell cycle, and apoptosis (11).

Neuronal inclusions, such as Lewy body–like hyaline inclusions (LBHIs), or the aggregation of mutant SOD1 in ALS1 (3, 12) are known to be important pathological features in the pathogenesis of neurodegenerative diseases. The TDP is a component of the ubiquitin-positive inclusions and neurites observed in frontotemporal dementia and ALS (13, 14). The TDP-positive round or filamentous inclusions in the cytoplasm and mislocalization of TDP from the nucleus to the cytoplasm have been observed in all cases of SALS (15) and FALS, but not in ALS1 (16, 17). A novel missense mutation in TDP was recently identified as causative in familial motor neuron disease and SALS (18, 19). Although the concept of TDP proteinopathy has been suggested (14, 20), the presence of TDP-positive inclusions in other diseases, including hippocampal sclerosis, Alzheimer disease (21), Parkinson disease (22), Pick disease (23), and neoplastic lesions (24), complicates this issue. Furthermore, Sanelli et al (25) have reported that TDP is not a major ubiquitinated target within the pathological inclusions of ALS.

From the Department of Neurology, Osaka University Graduate School of Medicine (HS, ME, SS), Yamadaoka, Suita; Department of Neuropathology, Institute of Neurological Sciences, Faculty of Medicine, Tottori University (SK), Nishi-cho, Yonago; Department of Health Science, Osaka University Graduate School of Medicine (YM), Yamadaoka, Suita; and Department of Neurology, Toneyama National Hospital (HF), Toneyama, Toyonaka, Japan.

Send correspondence and reprint requests to: Hisae Sumi, MD, PhD, Department of Neurology, Osaka University Graduate School of Medicine, 2-2 Yamadaoka, Suita, 565-0871, Japan; E-mail: hasumi@neurol.med.osaka-u.ac.jp

This study was supported by the Health and Labor Sciences Research on Measures for Incurable Disease, Ministry on Health, Labor and Welfare of Japan.

TABLE. Clinical and Pathological Data*

Patients	Age, years	Disease Duration, years	Initial Weakness Manifestation	Use of Respirator (Estimated Duration)	Cause of Death	Family History	No. Large Neurons†	No. Large Neurons With TDP Mislocalization†	No. Neuronal Inclusions†	No. Glial Inclusions†
SALS r-1	69	0.7	L	No	Pneumonia	No	13	6 (I)	40	16
SALS r-2	77	0.8	U	No	Resp. f.	No	23	8 (I>D)	34	4
SALS r-3	49	0.8	L, B	No	Resp. f.	No	9	4 (I)	35	6
SALS r-4	60	1.5	B, U	No	Pneumonia	No	36	12 (D>I)	25	38
SALS r-5	59	1.5	U	No	Resp. f.	No	16	9 (D>I)	12	22
SALS r-6	69	2	B, U	No	Resp. f.	No	22	12 (D>I)	25	38
SALS r-7	51	2	B	No	Resp. f.	No	22	11 (D>I)	21	11
SALS r-8	71	2	U	No	Resp. f.	No	21	4 (I>D)	69	8
SALS r-9	61	2	U	No	Resp. f.	No	8	3 (I>D)	12	9
SALS r-10	64	2	L	No	Pneumonia	No	7	0	9	123
SALS r-11	73	2.5	B	No	Resp. f.	No	25	4 (I>D)	14	7
SALS r-12	60	2.5	B, U	No	Resp. f.	No	12	7 (D>I)	18	19
SALS r-13	71	2.5	U	No	Resp. f.	No	4	0	26	26
SALS s-1	79	5	U	No	Resp. f.	No	2	0	0	0
SALS s-2	53	5.5	U	No	Resp. f.	No	9	0	4	2
SALS s-3	63	5.5	U, L	No	Resp. f.	No	4	0	2	2
SALS s-4	48	6.7	?	No	Resp. f.	No	15	0	0	2
SALS s-5	45	7.3	?	No	Resp. f.	No	2	0	0	3
				Median (range), 62 (45–79); 2.0 (0.7–7.3)						
ALS1-1 (C111Y)	71	7	L	3 years	Ren f.	Yes	0	0	20	31
ALS1-2 (126 2bp del)	42	2	L	0.5 years	Pneumonia	Yes	3	1 (D)	0	0
ALS1-3 (126 2bp del)	65	11	L	10 years	Hemorrhage	Yes	0	0	0	0
ALS1-4 (G37R)	50	9	U	2.5 years	Pneumonia	Yes	1	0	0	0
ALS1-5 (L126S)	67	9	L	No	Resp. f.	Yes	13	0	0	0
ALS1-6 (L126S)	45	8.5	L	No	Resp. f.	Yes	7	0	0	0
				Median (range), 58 (42–71); 9 (2–11)						

*ALS1, amyotrophic lateral sclerosis (*SOD-1* gene mutation); B, bulbar; D, diffuse staining pattern; D > I, predominantly diffuse staining pattern; I, inclusion pattern; I > D, predominantly inclusion pattern; L, lower limb; Ren. f., renal failure; Resp. f., respiratory failure; SALS *r*, sporadic ALS with a rapid clinical course (i.e. ≤2.5 years); SALS s, SALS with a slow clinical course; U, upper limb.

†Large neurons with cytoplasm exceeding 37 μm in diameter and clear nucleoli were counted. TAR DNA binding protein (TDP) mislocalization includes a diffuse staining pattern in the cytoplasm (D) and TDP-positive inclusions in the cytoplasm (I). Cell types containing TDP-positive inclusions were estimated as neuronal or glial on the basis of the morphology of their nuclei and cytoplasm.

To clarify how TDP may be involved in pathogenetic mechanisms in ALS, we examined SALS and ALS1 patients clinically and pathologically by immunohistochemistry using an anti-TDP antibody. We also examined the lumbar spinal cords of mutant SOD1 transgenic mice (G93A mice) that have lower copy numbers of the mutant *SOD1* gene than the G93A mice previously examined by Robertson et al (26); G93A mice with low copy numbers of the mutant *SOD1* gene show pathological changes that are similar to those in patients with ALS (27).

MATERIALS AND METHODS

ALS Cases and Pathological Assessment

Fixed paraffin-embedded 4-μm-thick sections through the lumbar spinal cord at the L5 level were obtained from Osaka University Graduate School of Medicine (Suita) for clinicopathologic analysis. These patients had SALS (n = 18; age at death 62 [median, 45–79] years; disease duration, 2 [0.7–7.3] years) or ALS1 (n = 6; age at death, 58 [42–71] years; disease duration, 9 [2–11] years; Table). All neuropathologic analyses were performed by trained neuropathologists. Sporadic ALS patients who did and did not have a history of respirator use and whose deaths were caused by respiratory failure or pneumonia were examined. Clinical data including the localization of initial symptoms, history of respirator use, cause of death, and family history are shown in the Table.

Deparaffinized sections were incubated for 30 minutes with 0.3% hydrogen peroxide to quench endogenous peroxidase activity and then washed with PBS. The primary antibodies used were rabbit polyclonal antibodies against TDP-43 (1:3000, Protein Tech Group, Chicago, IL) and ubiquitin (1:2000, Dako, Glostrup, Denmark), mouse monoclonal antibodies against human SOD1 (0.5 μg/mL, clone 1G2, MBL, Aichi, Japan) and phosphorylated neurofilament (1:10,000, SMI31, Covance, Berkeley, CA), and a sheep polyclonal antibody against human SOD1 (1:20,000, Calbiochem, San Diego, CA); these were applied to serial sections as primary antibodies. Goat anti-rabbit and anti-mouse immunoglobulins conjugated to peroxidase-labeled dextran polymer (ready to use, Dako Envision+, Dako Corp, Carpinteria, CA) and rabbit anti-sheep immunoglobulin (1:1000, Abcam PLC, Cambridge, United Kingdom) were used as secondary antibodies. Reaction products were visualized with 3,3′-diaminobenzidine tetrahydrochloride (ImmPACT DAB, Vector Laboratories, Burlingame, CA), and hematoxylin was used to counterstain cell nuclei.

To estimate the numbers of TDP-positive cytoplasmic inclusions, large neurons that had clear nucleoli and cell bodies with a diameter greater than 37 μm (28) (presumed to be α motoneurons) and the numbers of neurons with TDP mislocalization from the nucleus to the cytoplasm in the gray matter, from video images of each section obtained with a digital camera (Keyence VB-7010, Keyence, Osaka) attached to a light microscope (EclipseE800, Nikon, Tokyo), were counted. The diameters of the neurons were measured with the aid of image analysis software (VH-H1A5, Keyence). Mislocalization of TDP was defined as the presence of a TDP-negative nucleus and TDP-positive cytoplasm. In mislocalizations of TDP, there can also be diffuse staining patterns in the cytoplasm and TDP-positive filamentous or round inclusions in the cytoplasm. Cells containing TDP-positive inclusions were classified as neurons or glia on the basis of the shape of their nuclei and cytoplasm.

Animals

Transgenic mice expressing the mutated human *SOD1* (G93A) gene at a low level (B6SJL-TgN[SOD1]-G93A)1Gur^{dl} [G1L]) were obtained from Jackson Laboratory (Bar Harbor, ME). These mice carry 18 transgene copies because of a reduction in the copy number compared with (B6SJL-TgN[SOD1]-G93A)1Gur (G1H) mice, which express 25 copies (3). The G1L mice were bred and maintained as hemizygotes by mating with wild-type B6.SJL mice. Non-transgenic littermates were used as controls. All animals were genotyped and handled as previously described (29). We examined control (n = 6,292 [median, 240–296] days old) and G1L (n = 9,256 [224–281] days old, end stage) mice. One G1H mouse (120 days, end stage), also obtained from Jackson Laboratory, was examined to confirm the lack of TDP-43 abnormalities reported previously (26). *End stage* was defined as occurring when the mouse was so severely paralyzed that it could hardly move or drink water. The mice were killed with an overdose of sodium pentobarbital and perfused with PBS followed by 4% paraformaldehyde. The lumbar enlargement of the spinal cord was removed, immersed in 4% paraformaldehyde overnight at 4°C, and then dehydrated and embedded in paraffin blocks. Paraffin sections, 4-μm-thick, were prepared and stained with hematoxylin and eosin. Every fifth section (cut at 20-μm intervals) was obtained, and 4 sections from each mouse were used to count the total number of LBHIs in the sections. For immunohistochemistry, the primary antibodies used on the serial sections were against TDP-43 (1:600, Protein Tech Group) and human SOD1 (0.5 μg/mL, clone 1G2, MBL, Nagoya, Japan).

Semiquantitative Analysis of Immunoreactivity for TDP

Because variation in the TDP immunoreactivity (TDP-IR) was evident among G1L mice, the patterns of TDP immunostaining were divided into normal (0) and abnormal (1 to 4), the latter showing TDP-positive neurites and inclusions and varying degrees of nuclear positivity. The stages of normal or abnormal patterns were classified by TDP-IR of the neuron nuclei as follows: normal pattern (Stage 0): same as in normal littermates, with immunoreactivity apparent only in nuclei; abnormal pattern (Stages 1–4): Stage 1, weak immunoreactivity in nuclei; Stage 2, weak to moderate immunoreactivity in nuclei; Stage 3, moderate to strong immunoreactivity in nuclei; Stage 4, strong immunoreactivity in nuclei.

Quantitative Analysis of LBHIs

The numbers of LBHIs with a core and halo in neurons of the lumbar spinal cord were counted in hematoxylin and

eosin–stained sections (100× objective) from each G1L mouse as previously described (29).

Statistical Analysis

Differences in the numbers of TDP-positive inclusions in neurons and glia and in large neurons (>37 μm) between SALS patients with a rapid course and those with a slow course were analyzed by Wilcoxon rank sum test. The relationships among the numbers of large neurons and TDP-positive inclusions in neurons and glia were also analyzed using Spearman correlation coefficient with a 95% confidence interval (CI). In G1L mice, the relationships among age at the end stage, number of LBHIs, and TDP-IR were analyzed using Spearman correlation coefficient with 95% CI. Exploratory subgroup analyses for age at the end stage were done in the TDP-IR weak groups (Stages 1 and 2) and the TDP-IR strong groups (Stages 3 and 4) by Kolmogorov-Smirnov test. All statistical analyses were performed with SAS version 9.1 (SAS Institute Inc, Cary, NC).

RESULTS

ALS Cases

In the lumbar cords of SALS patients with disease durations less than or equal to 2.5 years (SALS r-1 to -13), mislocalization of TDP was frequently observed (Figs. 1B, C; Table); this was not evident in controls (Fig. 1A). There was a diffuse cytoplasmic staining pattern, especially in large neurons (>37 μm, Fig. 1B) and TDP-positive filamentous or round inclusions were evident in atrophic neurons and in glia (Figs. 1C, D); the nuclei in the neurons and glia were negative for TDP. In SALS patients with mild to moderate neuronal loss, there was often a diffuse TDP staining pattern in the cytoplasm of large neurons (Table). No extracellular TDP-positive inclusions were apparent. By contrast, in SALS patients with disease durations longer than 5 years (SALS s-1 to -5), neurons with diffuse cytoplasmic staining patterns were not evident, and TDP-positive inclusions were only rarely detected (Table). The TDP-IR of the nuclei of residual neurons appeared to be preserved.

In ALS1 patients, diffuse cytoplasmic TDP staining of large neurons was found only in 1 patient, i.e. ALS1-2 (126 2bp del), who had a clinical course of 2 years (Table). Some small neurons in Patients ALS1-2 and ALS1-3 (126 2bp del) also showed diffuse cytoplasmic TDP staining (Figs. 3A, C). The TDP-positive inclusions were prominent in the glia and in small neurons or their neurites in Patient ALS1-1 (C111Y), who had no remaining large neurons. The nuclei of cells with TDP-positive inclusions were TDP negative (Figs. 2A, E). Colocalization of TDP and SOD1 was frequently evident as

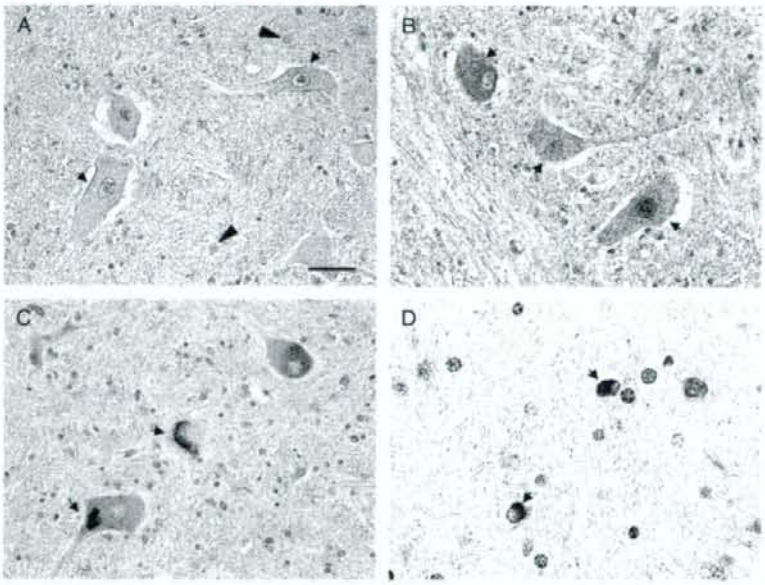

FIGURE 1. Mislocalization of TAR DNA binding protein (TDP) in cases of sporadic amyotrophic lateral sclerosis (SALS) with rapid clinical courses. **(A)** Normal control. The nuclei of large neurons are positive for TDP (arrows). Some glia (arrowheads) are weakly stained. **(B–D)** SALS patients. **(B)** There is diffuse punctate cytoplasmic staining in the neuron on the left (arrow), and heterogeneous staining in the middle (arrow) is observed in the cytoplasm. Nuclei of neurons on the left and in the middle are negative for TDP, whereas the nucleus of the neuron on the right is stained. **(C)** Variable appearances of cytoplasmic TDP inclusions (arrows). The structure on the left (arrow) is rounded, whereas the one in the middle neuron is elongated and filamentous (arrow). **(D)** Glial inclusions are positive for TDP (arrows). Immunohistochemistry against TDP. Scale bar = 50 μm.